Random Processes, Correlation, Power Spectral Density, Threshold Exceedance

CEE 541. Structural Dynamics

Duke University, Fall 2020

1 Random Processes

A random process $X(t)$ is a set (or "ensemble") of random variables expressed as a function of time (and/or some other independent variables).

$$X(t) = \left[\begin{array}{c} X_1(t) \\ X_2(t) \\ \vdots \\ X_m(t) \end{array} \right]$$

For example, if $X(t)$ represents be the wind at the top of the Cape Hatteras light house from 12:00 pm to 1:00 pm, then $X_j(t)$ could be the wind speed at the top of the Cape Hatteras light house from 12:00 pm to 1:00 pm on the j^{th} day of the year.

1.1 Ensemble Average

The *ensemble average* is the average across the variables in the ensemble at a fixed point in time, t.

$$\mathbb{E}[g(X(t))] = \mathbb{E}[g(X_1(t)), g(X_2(t)), \cdots, g(X_m(t))] \approx \frac{1}{m}\sum_{j=1}^{m} g(X_j(t))$$

In general the ensemble average can change with time. A random process X is *stationary* if ensemble statistics are equal for every point in time:

$$\mathbb{E}[g(X(t_1))] = \mathbb{E}[g(X(t_2))] \ \forall \ t_1, t_2$$

A process is *weak-sense stationary* if the first two moments of the probability density $f_X(X(t))$ are time-independent. A process is *strong-sense stationary* if all moments of the probability density $f_X(X(t))$ are time-independent.

1.2 Time Average

The *time average* is the average along time for a variable $X_j(t)$ in the ensemble.

$$\langle g(X_j) \rangle = \lim_{T\to\infty} \frac{1}{T} \int_{-T/2}^{T/2} g(X_j(t)) \ dt$$

1.3 Ergodic processes

A random process X is *ergodic* if its ensemble averages equal its time averages:

$$\mathbb{E}[g(X(t_i))] = \langle g(X_j) \rangle \ \forall \ i, j$$

Ergodic processes are stationary.

The statistics of an ergodic process $X(t)$ can be found from any single record $X_j(t)$ from the ensemble.

- mean value

$$\langle X(t) \rangle = \mathbb{E}[X(t)] = \lim_{T\to\infty} \frac{1}{T} \int_{-T/2}^{T/2} X_j(t) \ dt = \lim_{n\to\infty} \frac{1}{n} \sum_{i=1}^{n} x_j(t_i)$$

- mean-square value

$$\left\langle X^2(t) \right\rangle = \mathbb{E}[X^2(t)] = \lim_{T\to\infty} \frac{1}{T} \int_{-T/2}^{T/2} X_j^2(t) \ dt = \lim_{n\to\infty} \frac{1}{n} \sum_{i=1}^{n} x_j^2(t_i)$$

- variance

$$\sigma_X^2 = \mathbb{E}[X^2] - (\mathbb{E}[X])^2$$

Means and variances of the samples drawn *across the ensembles* shown in Figures 1 and 2 at different points in time are shown below.

Table 1. Sample means of the stationary and ergodic processes

process	2.00 s	4.00 s	6.00 s	7.00 s	8.00 s
ergodic	-0.02095	0.16549	-0.12142	0.06562	0.01531
stationary	-0.13769	-0.26535	-0.14263	0.15817	0.34448

Table 2. Sample variances of the stationary and ergodic processes

process	2.00 s	4.00 s	6.00 s	7.00 s	8.00 s
ergodic	1.2560	1.1429	0.9906	1.2514	1.0169
stationary	4.2568	4.0857	9.6974	2.3515	4.4192

The standard deviation of the mean, σ_μ is $\sigma/\sqrt{100} \approx 1/10 = 0.1$; the values of the ensemble means for the ergodic process are within 1 σ_μ of each other.

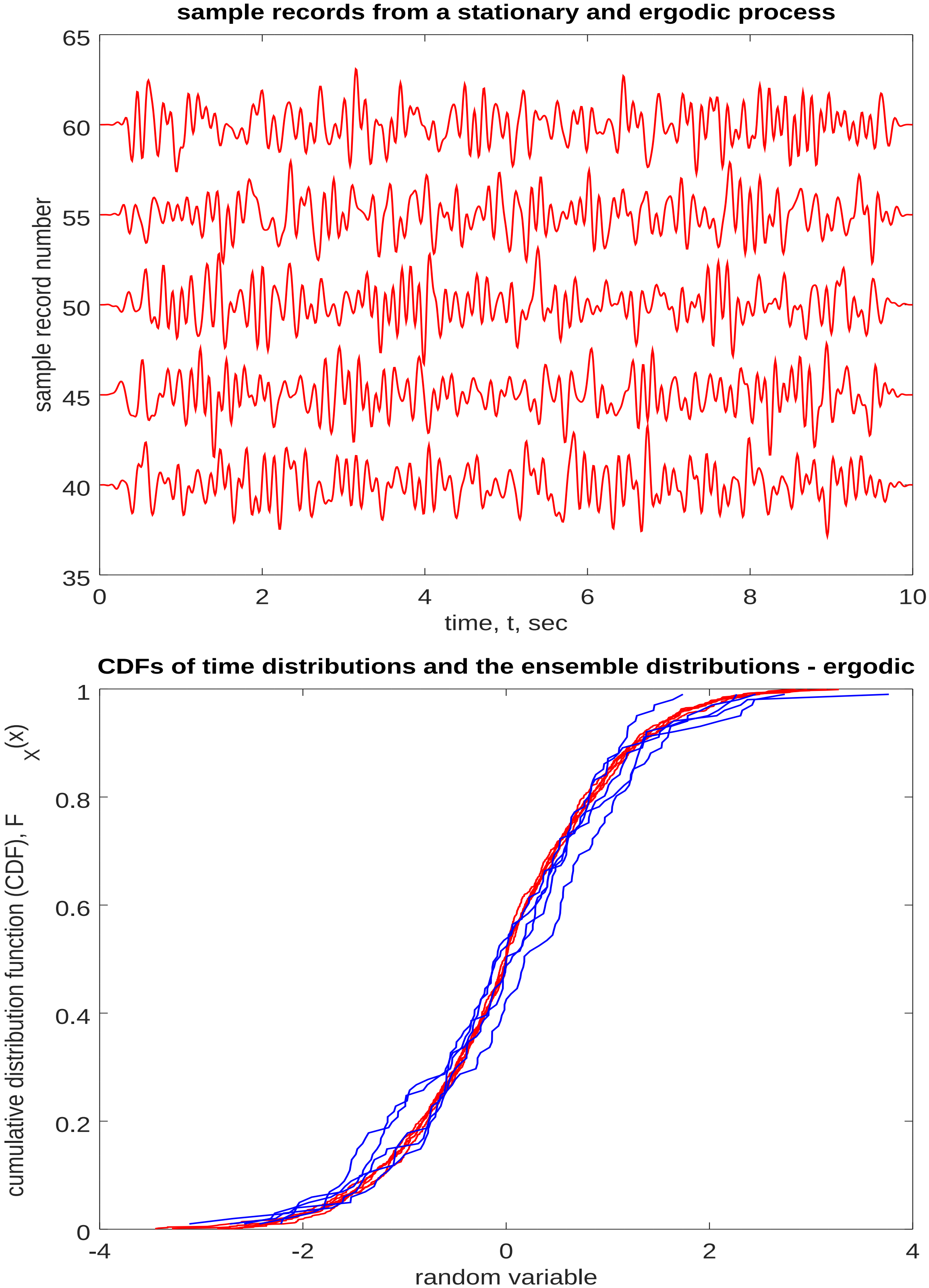

Figure 1. Samples of an ergodic random process

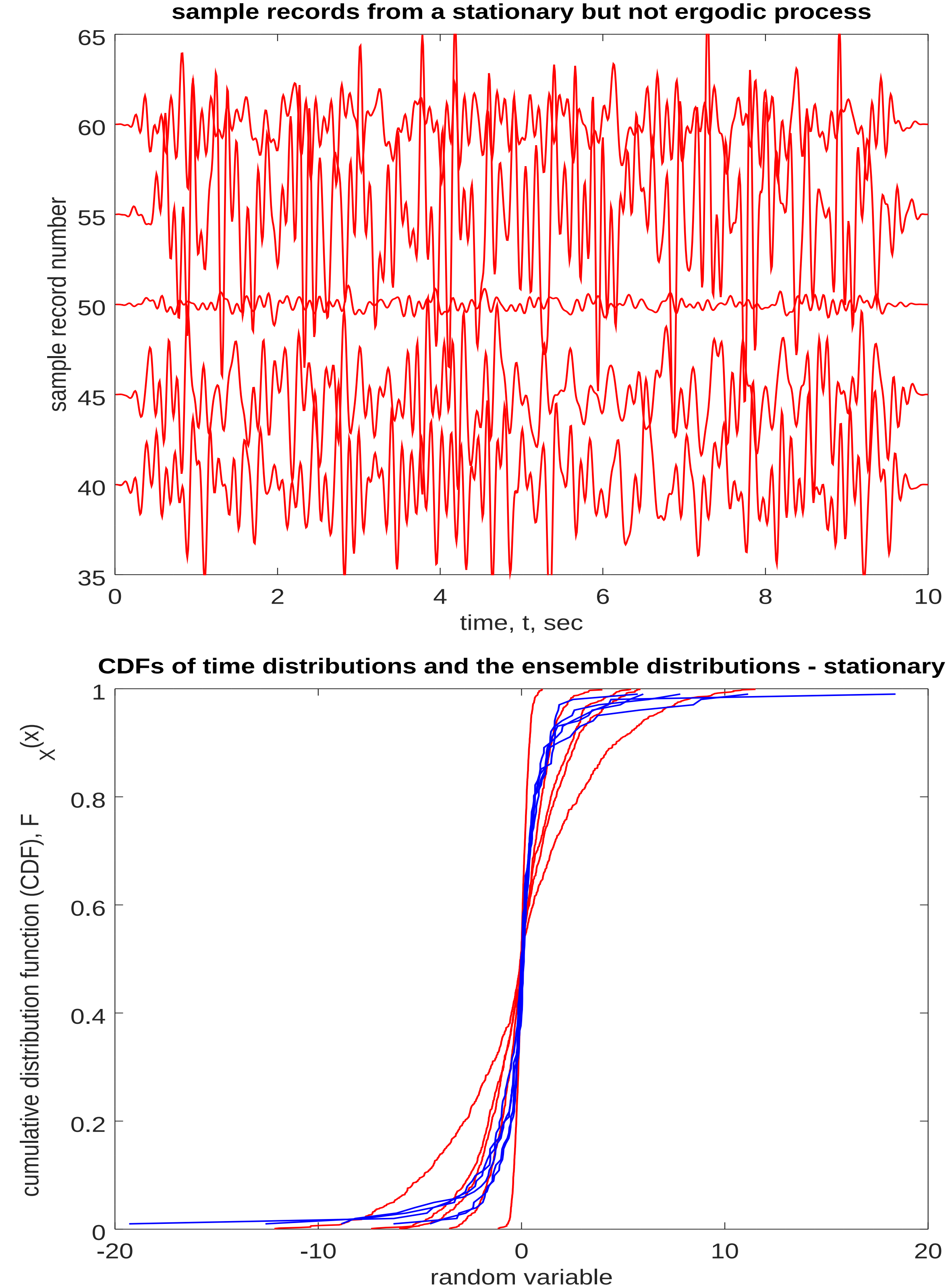

Figure 2. Samples of a stationary (but not ergodic) random process

2 The Fourier Transform Pair and the Dirac delta function

Recall the Fourier transform pair, [4]

$$\begin{aligned} x(t) &= \int_{-\infty}^{\infty} \bar{X}(f)\ \exp(+\mathrm{i}2\pi f t)\ df \\ \bar{X}(f) &= \int_{-\infty}^{\infty} x(t)\ \ \exp(-\mathrm{i}2\pi f t)\ dt \end{aligned}$$

If $x(t)$ is complex, then

$$x^*(t) = \int_{-\infty}^{\infty} \bar{X}^*(f)\ \exp(-\mathrm{i}2\pi f t)\ df$$

If $x(t)$ is real, then $\bar{X}(f) = \bar{X}^*(-f)$.

Recall the property of the Dirac delta function, $\delta(t)$,

$$\int_{-\infty}^{\infty} \delta(t - t')x(t')dt' = x(t)$$

and apply the forward and inverse Fourier transforms to $x(t)$,

$$\begin{aligned} x(t) &= \int_{-\infty}^{\infty} \left(\int_{-\infty}^{\infty} x(t') e^{-\mathrm{i}2\pi f t'} dt' \right) e^{+\mathrm{i}2\pi f t} df \\ &= \int_{-\infty}^{\infty} \left(\int_{-\infty}^{\infty} e^{\mathrm{i}2\pi f (t-t')} df \right) x(t')\ dt' \\ &= \int_{-\infty}^{\infty} \delta(t - t')\ x(t')\ dt' \end{aligned}$$

So the unit Dirac delta function has a unit Fourier spectrum.

$$\delta(t - t') = \int_{-\infty}^{\infty} (1) e^{+\mathrm{i}2\pi f (t-t')} df\ ,$$

A similar relation can be found by applying the Fourier transforms in the opposite order, and gives the Fourier transform of $x(t) = (1)\cos(2\pi f' t)$.

$$\delta(f \pm f') = \int_{-\infty}^{\infty} (1) e^{-\mathrm{i}2\pi (f \pm f') t} dt\ .$$

3 Parseval's Theorem

For (generally) complex-valued functions $x(t)$,

$$\int_{-\infty}^{\infty} x_1^*(t) x_2(t) \; dt = \int_{-\infty}^{\infty} \bar{X}_1^*(f) \bar{X}_2(f) \; df$$

The proof of Parseval's theorem involves the Fourier transform of the Dirac delta function:

$$\begin{aligned}
\int_{-\infty}^{\infty} x_1^*(t) x_2(t) \; dt &= \int_{-\infty}^{\infty} \left(\int_{-\infty}^{\infty} \bar{X}_1^*(f) e^{-\mathrm{i}2\pi f t} df \right) \left(\int_{-\infty}^{\infty} \bar{X}_2(f) e^{+\mathrm{i}2\pi f' t} df' \right) dt \\
&= \int_{-\infty}^{\infty} \int_{-\infty}^{\infty} \int_{-\infty}^{\infty} \bar{X}_1^*(f) \bar{X}_2(f') \; e^{+\mathrm{i}2\pi f t} \; e^{-\mathrm{i}2\pi f' t} \; df \; df' \; dt \\
&= \int_{-\infty}^{\infty} \int_{-\infty}^{\infty} \bar{X}_1^*(f) \bar{X}_2(f') \left(\int_{-\infty}^{\infty} e^{\mathrm{i}2\pi (f'-f) t} dt \right) df' \; df \\
&= \int_{-\infty}^{\infty} \int_{-\infty}^{\infty} \bar{X}_1^*(f) \bar{X}_2(f') \; \delta(f'-f) \; df' \; df \\
&= \int_{-\infty}^{\infty} \bar{X}_1^*(f) \left(\int_{-\infty}^{\infty} \bar{X}_2(f') \; \delta(f'-f) \; df' \right) df \\
&= \int_{-\infty}^{\infty} \bar{X}_1^*(f) \bar{X}_2(f) \; df
\end{aligned}$$

If $x_1(t)$ and $x_2(t)$ are both real, then $x_1^*(t) = x_1(t)$ but $\bar{X}_1^*(f) \neq \bar{X}_1(f)$, so,

$$\int_{-\infty}^{\infty} x_1(t) x_2(t) \; dt = \int_{-\infty}^{\infty} \bar{X}_1^*(f) \bar{X}_2(f) \; df$$

and further, if $x(t) = x_1(t) = x_2(t)$,

$$\int_{-\infty}^{\infty} x^2(t) \; dt = \int_{-\infty}^{\infty} \bar{X}^*(f) \bar{X}(f) \; df = \int_{-\infty}^{\infty} |\bar{X}(f)|^2 \; df$$

4 Auto-correlation

For a zero-mean process X ($\mathbb{E}[X_j(t)] = 0 \;\forall\; j$), the covariance of the process at time t, $X(t)$, with the process at time $t+\tau$, $X(t+\tau)$, is

$$R_{XX}(\tau) = \langle X(t)X(t+\tau)\rangle = \mathbb{E}[X(t)\cdot X(t+\tau)] \;=\; \lim_{T\to\infty}\frac{1}{T}\int_{-T/2}^{T/2} x(t)\cdot x(t+\tau)\;dt$$
$$= \lim_{n\to\infty}\frac{1}{n+1}\sum_{i=1}^{n} x(t_i)\cdot x(t_i+\tau)$$

If X is ergodic ($\mathbb{E}[g(X_j(t_1)] = \mathbb{E}[g(X_j(t_2)] \;\forall\; j, t_1, t_2$), then R_{XX} is independent of time t.

Since X is zero-mean by assumption, then $\mathbb{E}[X^2(t)] = \sigma_X^2$ and $R_{XX}(0)$ is the variance, σ_X^2.

The auto-correlation function is symmetric: $R_{XX}(-\tau) = R_{XX}(\tau)$, and $|R_{XX}(\tau)| \le R_{XX}(0)$.

An auto-correlation functions can be computed from the samples drawn *along the time series*, for the each of the 100 time records in the ensemble. The auto-correlation function for an ergodic process may be estimated from any of the sample records. Viewing auto-correlations from all of the records, above, gives an idea of the uncertainty in the auto-correlation function computed from records of finite-duration.

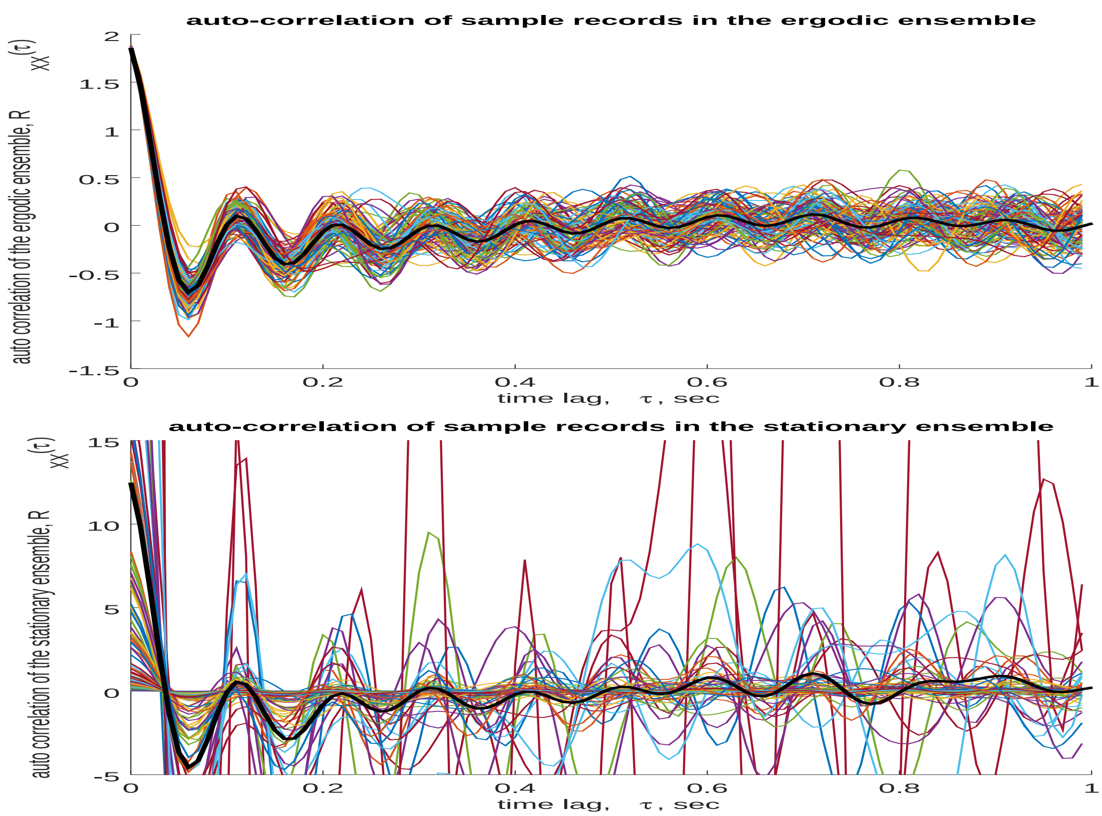

Figure 3. auto-correlation function for each of the time series in the ergodic and stationary ensembles.

4.1 Auto Power Spectral Density

The auto power spectral density $S_{XX}(f)$ of a zero-mean random process $x(t)$ is defined in terms of finite-duration Fourier transforms,

$$S_{XX}(f) = \lim_{T\to\infty} \mathbb{E}\left[\frac{1}{T} \left(\int_{-T/2}^{T/2} x(t)e^{-\mathrm{i}2\pi ft}dt\right)^{*} \left(\int_{-T/2}^{T/2} x(t)e^{-\mathrm{i}2\pi ft}dt\right)\right]$$

and has the following three properties:

- $$\int_{-\infty}^{\infty} S_{XX}(f)\ df = \left\langle X^2(t)\right\rangle$$

  proof:

$$\begin{aligned}
\int_{-\infty}^{\infty} S_{XX}(f)\ df &= \int_{-\infty}^{\infty} \lim_{T\to\infty} \mathbb{E}\left[\frac{1}{T} \left(\int_{-T/2}^{T/2} x(t)e^{-\mathrm{i}2\pi ft}dt\right)^{*} \left(\int_{-T/2}^{T/2} x(t)e^{-\mathrm{i}2\pi ft}dt\right)\right] df \\
&= \int_{-\infty}^{\infty} \lim_{T\to\infty} \mathbb{E}\left[\frac{1}{T} \int_{-T/2}^{T/2}\int_{-T/2}^{T/2} x^*(p)x(q)\ e^{+\mathrm{i}2\pi fp}\ e^{-\mathrm{i}2\pi fq}\ dp\ dq\right] df \\
&= \lim_{T\to\infty} \frac{1}{T}\ \mathbb{E}\left[\int_{-T/2}^{T/2}\int_{-T/2}^{T/2}\int_{-\infty}^{\infty} x^*(p)x(q)\ e^{+\mathrm{i}2\pi f(p-q)}\ df\ dp\ dq\right] \\
&= \lim_{T\to\infty} \frac{1}{T}\ \mathbb{E}\left[\int_{-T/2}^{T/2}\int_{-T/2}^{T/2} x^*(p)x(q) \left(\int_{-\infty}^{\infty} e^{+\mathrm{i}2\pi f(p-q)}\ df\right)\ dp\ dq\right] \\
&= \lim_{T\to\infty} \frac{1}{T}\ \mathbb{E}\left[\int_{-T/2}^{T/2}\int_{-T/2}^{T/2} x^*(p)x(q)\ \delta(p-q)\ dp\ dq\right] \\
&= \lim_{T\to\infty} \frac{1}{T}\ \mathbb{E}\left[\int_{-T/2}^{T/2} x^*(t)\ x(t)\ dt\right] \\
&= \lim_{T\to\infty} \frac{1}{T} \int_{-T/2}^{T/2} x^*(t)\ x(t)\ dt \quad = \quad \left\langle X^2(t)\right\rangle
\end{aligned}$$

- $$\int_{-\infty}^{\infty} S_{XX}(f)\ \exp(+\mathrm{i}2\pi f\tau)\ df = R_{XX}(\tau)$$

  proof:

$$\begin{aligned}
\int_{-\infty}^{\infty} S_{XX}(f) e^{+\mathrm{i}2\pi f\tau}\ df &= \int_{-\infty}^{\infty} \lim_{T\to\infty} \mathbb{E}\left[\frac{1}{T}\ \left(\int_{-T/2}^{T/2} x(t) e^{-\mathrm{i}2\pi f t} dt\right)^* \left(\int_{-T/2}^{T/2} x(t) e^{-\mathrm{i}2\pi f t} dt\right)\right] e^{+\mathrm{i}2\pi f\tau}\ df \\
&= \int_{-\infty}^{\infty} \lim_{T\to\infty} \mathbb{E}\left[\frac{1}{T}\ \int_{-T/2}^{T/2}\int_{-T/2}^{T/2} x^*(p)x(q)\ e^{+\mathrm{i}2\pi f p}\ e^{-\mathrm{i}2\pi f q}\ dp\ dq\right] e^{+\mathrm{i}2\pi f\tau}\ df \\
&= \lim_{T\to\infty} \frac{1}{T}\ \mathbb{E}\left[\int_{-T/2}^{T/2}\int_{-T/2}^{T/2}\int_{-\infty}^{\infty} x^*(p)x(q)\ e^{+\mathrm{i}2\pi f(p-q+\tau)}\ df\ dp\ dq\right] \\
&= \lim_{T\to\infty} \frac{1}{T}\ \mathbb{E}\left[\int_{-T/2}^{T/2}\int_{-T/2}^{T/2} x^*(p)x(q) \left(\int_{-\infty}^{\infty} e^{+\mathrm{i}2\pi f(p-q+\tau)}\ df\right)\ dp\ dq\right] \\
&= \lim_{T\to\infty} \frac{1}{T}\ \mathbb{E}\left[\int_{-T/2}^{T/2}\int_{-T/2}^{T/2} x^*(p)x(q)\ \delta(p-q+\tau)\ dp\ dq\right] \\
&= \lim_{T\to\infty} \frac{1}{T}\ \mathbb{E}\left[\int_{-T/2}^{T/2} x^*(t)\ x(t+\tau)\ dt\right] \\
&= \lim_{T\to\infty} \frac{1}{T} \int_{-T/2}^{T/2} x^*(t)\ x(t+\tau)\ dt \quad = \quad R_{XX}(\tau)
\end{aligned}$$

- $$\int_{-\infty}^{\infty} R_{XX}(\tau)\ \exp(-\mathrm{i}2\pi f\tau)\ d\tau = S_{XX}(f)$$

  proof:

$$\begin{aligned}
\int_{-\infty}^{\infty} R_{XX}(\tau)\ e^{-\mathrm{i}2\pi f\tau}\ d\tau &= \int_{-\infty}^{\infty} \lim_{T\to\infty} \frac{1}{T}\ \mathbb{E}\left[\int_{-T/2}^{T/2} x^*(t)\ x(t+\tau)\ dt\right]\ e^{-\mathrm{i}2\pi f\tau}\ d\tau \\
&= \lim_{T\to\infty} \frac{1}{T}\ \mathbb{E}\left[\int_{-T/2}^{T/2}\int_{-T/2}^{T/2} x^*(t)\ x(t+\tau)\ e^{-\mathrm{i}2\pi f\tau}\ d\tau\ dt\right] \\
&= \lim_{T\to\infty} \frac{1}{T}\ \mathbb{E}\left[\int_{-T/2}^{T/2}\int_{-T/2}^{T/2} x^*(p)\ x(q)\ e^{+\mathrm{i}2\pi f(p-q)}\ dp\ dq\right] \\
&= \lim_{T\to\infty}\ \mathbb{E}\left[\frac{1}{T}\left(\int_{-T/2}^{T/2} x(p) e^{-\mathrm{i}2\pi f p}\ dp\right)^*\ \left(\int_{-T/2}^{T/2} x(q)\ e^{-\mathrm{i}2\pi f q}\ dq\right)\right] \\
&= S_{XX}(f)
\end{aligned}$$

  Thus, the auto-correlation function and the auto power spectrum are related by Fourier transform pairs. These are the *Wiener-Khintchine* relations.

Note that the power spectral density is a *density* function. If the process $X(t)$ has units of 'm' (meters), and the circular frequency, f, is the independent variable (with units of 'Hz' or 'cycles/sec'), then the units of of the power spectral density is $S_{XX}(f)$ is 'm^2/Hz'.

Alternatively, if the angular frequency ω is the independent variable ($d\omega = 2\pi\ df$), then the units of the power spectral density $S_{XX}(\omega)$ is 'm^2/(rad/s)'.

So, to convert between frequencies f and ω, the value of the power spectral density needs to be scaled as well.

$$S_{XX}(\omega)\ d\omega = 2\pi\ S_{XX}(f)\ df$$

4.2 One-sided Power Spectral Density

The one-sided power spectral density function $G_{XX}(\omega)$ is defined here so that

$$\left\langle X^2(t) \right\rangle = \int_0^\infty G_{XX}(f)\ df = \int_0^\infty G_{XX}(\omega/(2\pi)) \frac{df}{d\omega}\ d\omega = \frac{1}{2\pi} \int_0^\infty G_{XX}(\omega)\ d\omega$$

Since $S_{XX}(f)$ is symmetric about $f = 0$,

$$\left\langle X^2(t) \right\rangle = 2 \int_0^\infty S_{XX}(f)\ df\ ,$$

so, the one-sided psd $G_{XX}(f)$ is twice the symmetric, two-sided psd $S_{XX}(f)$

$$G_{XX}(|f|)\ df = 2\ S_{XX}(f)\ df$$

5 Cross-correlation

For zero-mean processes X and Y ($\mathbb{E}[X_i(t)] = 0$ and $\mathbb{E}[Y_j(t)] = 0\ \forall\ i, j$), the covariance of process X at time t, $X(t)$, with a different process Y at time $t + \tau$, $Y(t + \tau)$, is

$$\begin{aligned} R_{XY}(\tau) = \langle X(t)Y(t+\tau) \rangle = \mathbb{E}[X(t) \cdot Y(t+\tau)] \ &= \ \lim_{T\to\infty} \frac{1}{T} \int_{-T/2}^{T/2} x(t) \cdot y(t+\tau)\ dt \\ &= \ \lim_{n\to\infty} \frac{1}{n+1} \sum_{i=1}^{n} x(t_i) \cdot y(t_i+\tau) \end{aligned}$$

If X and Y are ergodic random processes ($\mathbb{E}[g(X(t_1)] = \mathbb{E}[g(X(t_2)]\ \forall\ t_1, t_2$ and $\mathbb{E}[g(Y(t_1)] = \mathbb{E}[g(Y(t_2)]\ \forall\ t_1, t_2$), then $R_{XY}(\tau)$ is independent of time.

Since X and Y are zero-mean random processes by assumption, then $R_{XY}(0) = \mathbb{E}[X(t)Y(t)]$ which is the covariance of X and Y, $\mathbb{V}[X, Y]$.

The cross-correlation function is *not* symmetric: $R_{XY}(-\tau) \neq R_{XY}(\tau)$,
however, $R_{XY}(\tau) = R_{YX}(-\tau)$.

5.1 Cross Power Spectral Density

The cross-power spectral density is defined as

$$S_{XY}(f) = \lim_{T\to\infty} \mathbb{E}\left[\frac{1}{T} \left(\int_{-T/2}^{T/2} x(t) e^{-\mathrm{i}2\pi f t} dt \right)^* \left(\int_{-T/2}^{T/2} y(t) e^{-\mathrm{i}2\pi f t} dt \right) \right] = S^*_{XY}(-f)$$

$$\begin{aligned} R_{XY}(\tau) &= \int_{-\infty}^{\infty} S_{XY}(f)\ \exp(+\mathrm{i}2\pi f\tau)\ df \\ S_{XY}(f) &= \int_{-\infty}^{\infty} R_{XY}(\tau)\ \exp(-\mathrm{i}2\pi f\tau)\ d\tau \quad \cdots \quad \text{Wiener – Khintchine} \end{aligned}$$

6 Derivitives of Auto-Correlations and Power Spectral Density of Derivitives

Recall

$$R_{XX}(\tau) = \langle X(t)X(t+\tau)\rangle = \mathbb{E}[X(t)\cdot X(t+\tau)]$$

So

$$\frac{d}{d\tau}R_{XX}(\tau) = R'_{XX}(\tau) = \left\langle X(t)\dot{X}(t+\tau)\right\rangle = \left\langle \dot{X}(t)X(t+\tau)\right\rangle$$

and

$$\frac{d^2}{d\tau^2}R_{XX}(\tau) = R''_{XX}(\tau) = -\left\langle \dot{X}(t)\dot{X}(t+\tau)\right\rangle = -R_{\dot{X}\dot{X}}(\tau)$$

Thus,

$$S_{\dot{X}\dot{X}}(f) = (f)^2\ S_{XX}(f) \quad \text{and} \quad S_{\ddot{X}\ddot{X}}(f) = (f)^4\ S_{XX}(f)$$

7 Spectral Moments and Spectral Bandwidth

Consider the moments of the two-sided power spectral density $S_{Y,Y}(f)$, λ_m is the m-th *spectral moment*,

$$\lambda_m = 2\int_0^\infty f^m\ S_{Y,Y}(f)\ df$$

So, the variance of Y and the variance of $\dot{Y}$ can be expressed in terms of moments of the power spectral densities,

$$\lambda_0 = \sigma_y^2 \equiv \left\langle y^2(t)\right\rangle$$

$$\lambda_2 = \sigma_{\dot{y}}^2 \equiv \left\langle \dot{y}^2(t)\right\rangle$$

From these moments, the *central frequency* $\bar{f}$ is defined as

$$\bar{f} = \sqrt{\frac{\lambda_2}{\lambda_0}}$$

and the *bandwidth factor* δ is defined as

$$\delta = \sqrt{1 - \frac{\lambda_1^2}{\lambda_0\lambda_2}}$$

Small values of the bandwidth factor correspond to *narrow band* processes, in which the power of the time series is concentrated around the central frequency.

For the displacement response of a lightly damped simple oscillator with natural frequency ω_n and damping ratio ζ, ,

$$\lambda_0 = \frac{\pi S_o}{4\zeta{\omega_\mathrm{n}}^2} = \sigma_y^2\ , \qquad \lambda_1 = \frac{{\omega_\mathrm{n}}^2}{\sqrt{{\omega_\mathrm{n}}^2(1-\zeta^2)}}\lambda_0\left[1 - \frac{1}{\pi}\tan^{-1}\left(\frac{2\zeta\sqrt{1-\zeta^2}}{1-2\zeta^2}\right)\right]\ , \qquad \lambda_2 = \frac{\pi S_o}{4\zeta\omega_\mathrm{n}}$$

and the bandwidth factor increases monotonically with the damping ratio, from $\delta = 0$ at $\zeta = 0$ to $\delta = 0.72$ at $\zeta = 1$. For $\zeta < 0.2$, $\delta^2 \approx (4\zeta/\pi)(1 - 1.1\zeta)$.

8 Examples

- Dirac delta function $x(t) = \delta(t)$

$$
\begin{aligned}
\bar{X}(f) = & \int_{-T/2}^{T/2} \delta(t) \ \exp(-i2\pi f t) \ dt & = 1 \\
S_{XX}(f) = & \lim_{T\to\infty} \mathbb{E}\left[\tfrac{1}{T}\bar{X}^*(f)\bar{X}(f)\right] & = 0 \\
R_{XX}(\tau) = & \int_{-\infty}^{\infty} S_{XX}(f) \ \exp(i2\pi f\tau) \ df & = 0 \\
R_{XX}(0) = & \int_{-\infty}^{\infty} \delta(t)^2 \ dt & = \infty
\end{aligned}
$$

- Gaussian pulse

$$
\begin{aligned}
x(t) &= \frac{1}{\sqrt{2\pi\sigma^2}} \ \exp\left[-\frac{1}{2}\left(\frac{t-\mu}{\sigma}\right)^2\right] \\
\bar{X}(f) &= \exp\left[-2\left((\pi\sigma f)^2 + i\pi\mu f\right)\right] \\
S_{XX}(f) &= \exp\left[-\left(2\pi\sigma f\right)^2\right] \\
R_{XX}(\tau) &= \frac{1}{\sqrt{4\pi\sigma^2}} \ \exp\left[-\left(\frac{\tau}{2\sigma}\right)^2\right]
\end{aligned}
$$

... $x(t)$, $\bar{X}(f)$, $S_{XX}(f)$, and $R_{XX}(\tau)$ are all Gaussian!

- Finite duration pulse

$$
\begin{aligned}
x(t) &= \begin{cases} 1-\cos(\pi t/T_p) & -T_p < t < T_p \\ 0 & t < -T_p, T_p < t \end{cases} \\
\bar{X}(f) &= \int_{-T_p}^{T_p} \cos(\pi t/T_p) \ \exp(-i2\pi f t) \ dt = \frac{2\sin(\pi f T_p)\cos(\pi f T_p)}{\pi f(1-4\pi f^2 T_p^2)}
\end{aligned}
$$

- Band-limited white noise

$$
\begin{aligned}
S_{XX}(f) &= \begin{cases} S_o & -f_c < f < f_c \\ 0 & f < -f_c, f_c < f \end{cases} \\
R_{XX}(\tau) &= \frac{1}{\pi f_c \tau} \sin(2\pi f_c \tau) \\
|\bar{X}(f)| &= \sqrt{2S_{XX}(f) \ df} \\
x(t) &= \int_0^{f_c} 2\sqrt{S_{xx}(f)df} \cos(2\pi f t + \theta(f))df. \\
x(t) &\approx \sum_{k=1}^{n/2} 2\sqrt{S_{XX}(f_k) \ \Delta f} \ \cos(2\pi f_k t + \theta(f_k))
\end{aligned}
$$

where $f_k = (k\Delta f)$ and θ is a random variable uniformly distributed between 0 and 2π.

9 Computation with discrete-time signals

```
% PowerSpectra.m --- H.P. Gavin --- 10 Nov 2014, 14 Dec 2016
 n = 1024;                        % number of points in the time-series
dt = 0.010;                       % time step increment, s
T  = n*dt;                        % duration of the time series, s
df = 1/T;                         % frequency increment, Hz

t = [ 0 : n/2 , -n/2+1 : -1]*dt;  % time values from -T/2+dt to T/2
f = [ 0 : n/2 , -n/2+1 : -1]*df;  % frequency values from -1/(2*dt) to +1/(2*dt)
idx = [ n/2+2:n , 1:n/2+1 ];      % resorting index for plots
tau = f * dt / df;                % time lag values

Example = 2                       % two examples
switch Example
% (1) given a time series [x(1) . . . x(n)] estimate Sxx(f)
% (2) given a power spectral density Sxx(f), synthesize a realization of [x(1) . . . x(n)]

 case 1  % given a time series  . . . for example . . .
  % a noisy two-tone signal
  x = sin(2*pi*6.18*t) + sin(2*pi*10.0*t) + 0.1 * randn(1,n) / sqrt(dt);

  % . . . compute the power spectral density from the time series
  X = fft(x) / n;                % complex Fourier coefficients from time series
  Sxx = conj(X) .* X / df;       % power spectral density from the time series

 case 2  % given a power spectral density . . . for example . . .
  % a positive two-sided power spectral density, symmetric about f=0 . . .
  Sxx = 1.0 ./ (1.0 + (f/10).^2 ).^2;

  % . . . synthesize a realization for the time series from the power spectral density
  % random phase angle at positive frequencies, uniformly-distributed between -pi and pi
  theta = 2*pi*rand(1,n/2) - pi;
  theta = [ 0 , theta , -theta(n/2-1:-1:1) ]; % phase angles anti-symmetric about f=0
  theta(n/2+1) = 0;                           % for real-valued signals
  x = real(ifft(sqrt(Sxx*df) .* exp(i*theta)))*n;   % imag part ~ 1e-16
end

% . . . compute the auto-correlation from the power-spectral density
Rxx = real(ifft(Sxx)) / dt;

% . . . compare mean-square calculations  . . .
format long
mean_square = sum(x.^2) * dt / T    % mean square  of  the time series
mean_square = sum(Sxx) * df         % mean square from the power spectral density
mean_square = Rxx(1)                % mean square from the auto-correlation
```

Referring to figures on the next page,

- Case 1: The presence of two sinusoidal components is impossible to discern from the time series. Two components at 10 Hz and 6.18 Hz are clearly apparent in the power spectrum.

  The spike in $R_{XX}(\tau)$ at $\tau = 0$ is from the added white noise, w.

  Two sinusoidal components are visibly present in the plot of $R_{XX}(\tau)$.

- Case 2: The time series contains a broad range of frequency components, with more spectral power at the low frequencies.

  The time series loses correlation at time lags τ greater than 0.1 s.

- The three mean square calculations give the same values in both cases.

Case 1 : a noisy two-tone signal

$$x(t_i) = \sin(2\pi(6.18)t_i) + \sin(2\pi(10.0)t_i) + 0.1w_i \quad \text{where} \quad w_i \quad \text{is unit Gaussian noise}$$

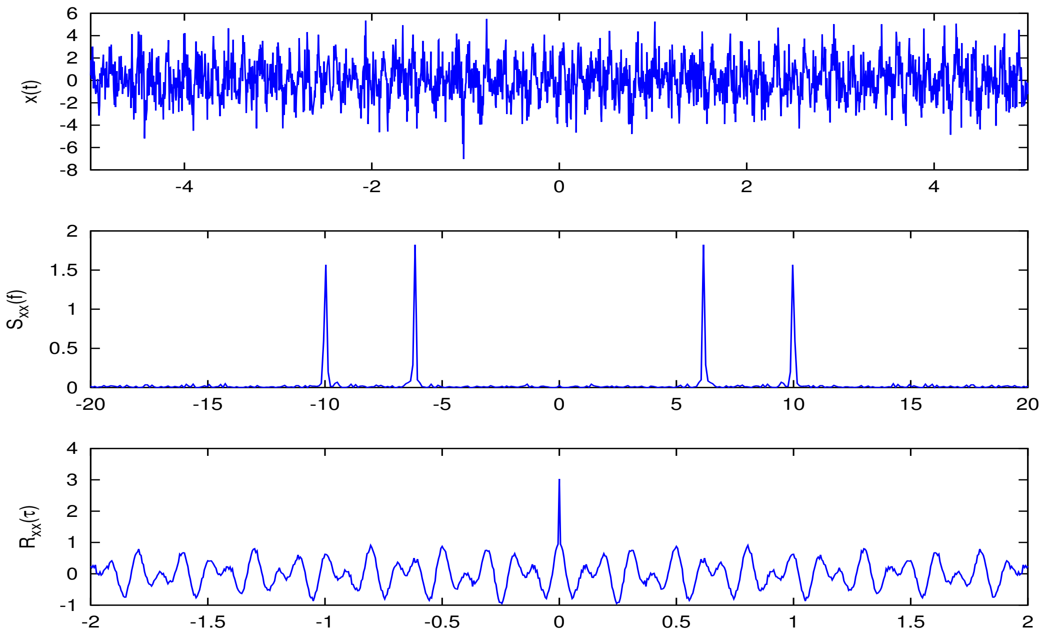

Case 2 : a positive two-sided power spectral density, symmetric about f=0

$$S_{XX}(f) = 1/(1 + (f/10)^2)^2$$

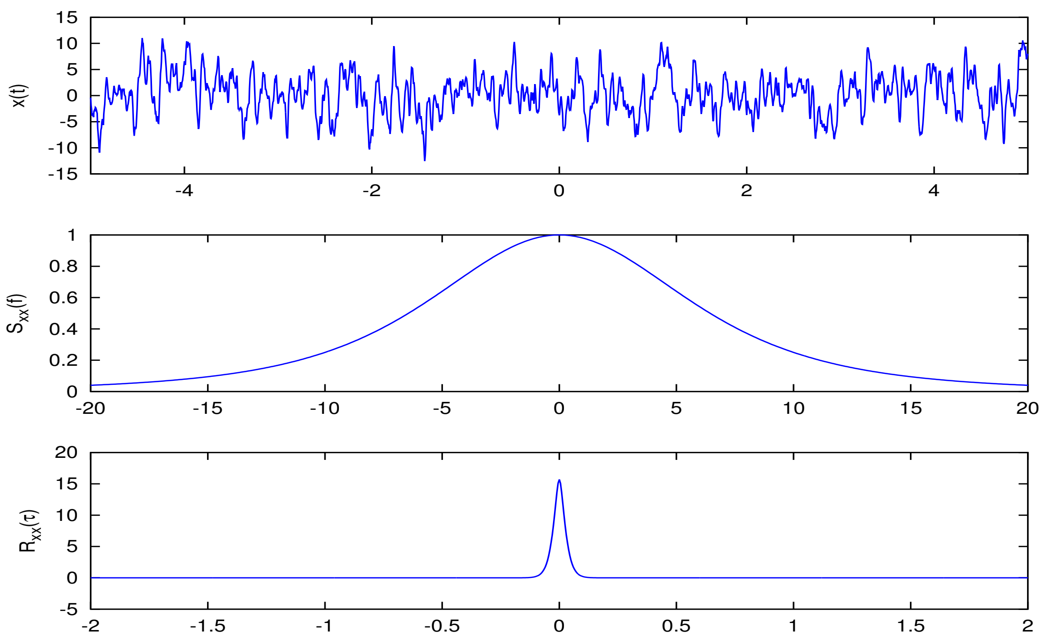

PSD_test.m   Fri Nov 20 10:36:13 2015   1

```
% test computations for
% Double-sided auto power spectral density
% Auto correlation function
% mean square value computed three ways

% note: correct scaling ...
%
%  df = 1 / (n*dt)
%
%  x  =  ifft(sqrt(S*df) .* exp(i*theta)) * n
%  X  =  fft(x) / n
%  S  =  conj(X).*X / df
%  R  =  ifft(S) / dt

 n = 4096;                     % # of points
dt = 0.010;                    % time step
T  = n*dt;                     % total time
df = 1/T;                      % frequency step

t  = [0:n/2 , -n/2+1:-1] * dt;   % time axis

f = [ 0:n/2 , -n/2+1:-1 ] * df;  % freqency axis

idx = [n/2+2:n, 1:n/2+1];        % re-sorting

tau = f * dt / df;               % time lag values

epsPlots = 0; formatPlot(epsPlots);
format long;         % a lot of significant figures

% ------------- example 1   .... "one+cosine" pulse

Tp = 1;                          % half-pulse period
x = 1+cos(pi*t/Tp);              % "one+cosine"
x(find(t < -Tp)) = 0;
x(find(t >  Tp)) = 0;

X = fft(x)/n;                    % Fourier coeff's

Sxx =  conj(X).*X/df;            % psd

Rxx = real(ifft(Sxx))/dt;        % auto correlation

mean_sq_A = sum(x.^2)*dt/T      % from x(t)
mean_sq_B = sum(Sxx)*df         % from Sxx(f)
mean_sq_C = Rxx(1)              % from Rxx(tau)

% All three mean_sq calculations are identical!

figure(1)
 clf
 subplot(311)
  plot(t(idx),x(idx))
  axis([-2 2 -0.1 2.1])
  ylabel('x(t)')
  text(-Tp, 0.2,'-T_p'); text( Tp, 0.2,'+T_p');
 subplot(312)
  plot(f(idx),Sxx(idx))
  axis([-2 2 -0.005 0.105])
  ylabel('S_{xx}(f)')
  text(-1/Tp, 0.01,'-1/T_p'); text( 1/Tp, 0.01,'+1/T_p');
 subplot(313)
  plot(tau(idx),Rxx(idx))
  axis([-2 2 -0.005 0.08])
  ylabel('R_{xx}(\tau)')
  text(-Tp, 0.003,'-T_p'); text( Tp, 0.003,'+T_p');
 if epsPlots, print('PSD1.eps','-color','-FHelvetica:10'); end

% ------------------------ example 1

% ----------- example 2   .... low-pass random noise

Fc = 2.5;                  % cut-off freqency, Hz
So = 1.25;                 % PSD value in pass-band
Sxx = So*ones(1,n);        % band-limitted noise
Sxx(find(f < -Fc)) = 0;
Sxx(find(f >  Fc)) = 0;



Rxx = real(ifft(Sxx))/dt;  % analytic auto-correlation

% synthesize a sample of data

x = zeros(1,n);              % x(t) built up by sums
theta = 2*pi*rand(1,n/2);    % random phase angle
theta = [ 0 , theta , -theta(n/2-1:-1:1) ];  % anti-symm.
theta(n/2+1) = 0;            % for real-valued signals
for k=1:n/2+1                % sum over freq's >=0 only
  x = x + 2*sqrt(Sxx(k)*df)*cos(2*pi*f(k)*t+theta(k));
  if (k==1) x = x/2; end % first Fourier coeff at f=0;
end

x_ifft = ( ifft(sqrt(Sxx*df) .* ...
                    (cos(theta) + i*sin(theta))) )*n;
imag_over_real = norm(imag(x_ifft))/norm(real(x_ifft))
x_ifft = real(x_ifft);

X_data = fft(x)/n;        % Fourier coeff's of data

Sxx_data =  conj(X_data).*X_data/df;  % Sxx of data

Rxx_data = real(ifft(Sxx_data))/dt;   % Rxx of data



mean_sq_A = sum(x_ifft.^2)*dt/T % from data         **
mean_sq_B = sum(Sxx)*df         % from analytic Sxx **
mean_sq_C = Rxx(1)              % from analytic Rxx **
mean_sq_D = sum(x.^2)*dt/T      % from data         *
mean_sq_E = sum(Sxx_data)*df    % from Sxx_data     *
mean_sq_F = Rxx_data(1)         % from Rxx_data     *

% All six mean_sq calculations are identical!

figure(2)
 clf
 subplot(311)
  plot(t(idx),x(idx), t(idx),x_ifft(idx),'-.r')
  axis([-20 20])
  ylabel('x(t)')
  legend('sum cosine','ifft')
 subplot(312)
  plot(f(idx),Sxx(idx), f(idx),Sxx_data(idx),'-.r')
  axis([-3 3 -0.1 2])
  ylabel('S_{xx}(f)')
  text(-2.5, 0.2,'-f_c'); text( 2.5, 0.2,'+f_c'); text( 0, 1.4,
'S_o');
  legend('model', 'data')
 subplot(313)
  plot(tau(idx),Rxx(idx),tau(idx),Rxx_data(idx),'-.r')
  axis([-2 2])
  set(gca,'xTick',[-4:4]/Fc);
  set(gca,'xTickLabel',['-4/f_c';'-3/f_c';'-2/f_c';'-1/f_c';'0'
;'+1/f_c';'+2/f_c';'+3/f_c';'+4/f_c']);
  ylabel('R_{xx}(\tau)')
  legend('model', 'data')
if epsPlots, print('PSD2.eps','-color','-FHelvetica:10'); end

% The Sxx from  FFT of x equals generating Sxx
% The Rxx from IFFT of S equals analytic Rxx

% ------------------------ example 2

% ----------- example 3   .... band-pass random noise

Flo = 0.5;               % low  cut-off frequency, Hz
Fhi = 2.5;               % high cut-off frequency, Hz
So = 1.25;               % two-sided pass band PSD
Sxx = So*ones(1,n);
Sxx(find(f < -Fhi)) = 0;
Sxx(find(f >  Fhi)) = 0;
Sxx(find(-Flo < f & f <  Flo)) = 0;

Rxx = real(ifft(Sxx))/dt;  % analytic auto-correlation

% synthesize a sample of data

x = zeros(1,n);              % x(t) built up by sums
theta = 2*pi*rand(1,n/2);    % random phase angle
theta = [ 0 , theta , -theta(n/2-1:-1:1) ];  % anti-symm.
theta(n/2+1) = 0;            % for real-valued signals
for k=1:n/2+1                % sum over freq's >=0 only
  x = x + 2*sqrt(Sxx(k)*df)*cos(2*pi*f(k)*t+theta(k));
% Sxx(f=0) = 0, so no need for the "x/2" line.
end

x_ifft = (ifft(sqrt(Sxx*df) .* exp(i*theta)))*n;

imag_over_real = norm(imag(x_ifft))/norm(real(x_ifft))
x_ifft = real(x_ifft);

X_data = fft(x)/n;        % Fourier coeff's of data

Sxx_data =  conj(X_data).*X_data/df;  % Sxx of data

Rxx_data = real(ifft(Sxx_data))/dt;   % Rxx of data



mean_sq_A = sum(x_ifft.^2)*dt/T % from data
mean_sq_B = sum(Sxx)*df         % from analytic Sxx
mean_sq_C = Rxx(1)              % from analytic Rxx
mean_sq_D = sum(x.^2)*dt/T      % from data
mean_sq_E = sum(Sxx_data)*df    % from Sxx_data
mean_sq_F = Rxx_data(1)         % from Rxx_data

% All six mean_sq calculations are identical!

figure(3)
 clf
 subplot(311)
  plot(t(idx),x(idx), t(idx), x_ifft(idx),'-.r')
  axis([-20 20])
  ylabel('x(t)')
  legend('sum cosine','ifft')
 subplot(312)
  plot(f(idx),Sxx(idx), f(idx),Sxx_data(idx),'-.r')
  axis([-3 3 -0.1 2])
  ylabel('S_{xx}(f)')
  text(-Fhi, 0.4,'-f_{hi}'); text( Fhi, 0.4,'+f_{hi}');
  text(-Flo, 0.4,'-f_{lo}'); text( Flo, 0.4,'+f_{lo}'); text( 0
, 1.4,'S_o');
  legend('model', 'data')
 subplot(313)
  plot(tau(idx),Rxx(idx),tau(idx),Rxx_data(idx),'-.r')
  axis([-2 2])
  ylabel('R_{xx}(\tau)')
  legend('model', 'data')
if epsPlots, print('PSD3.eps','-color','-FHelvetica:10'); end

% The Sxx from  FFT of x equals generating Sxx
% The Rxx from IFFT of S equals analytic Rxx

% ------------------------ example 3
```

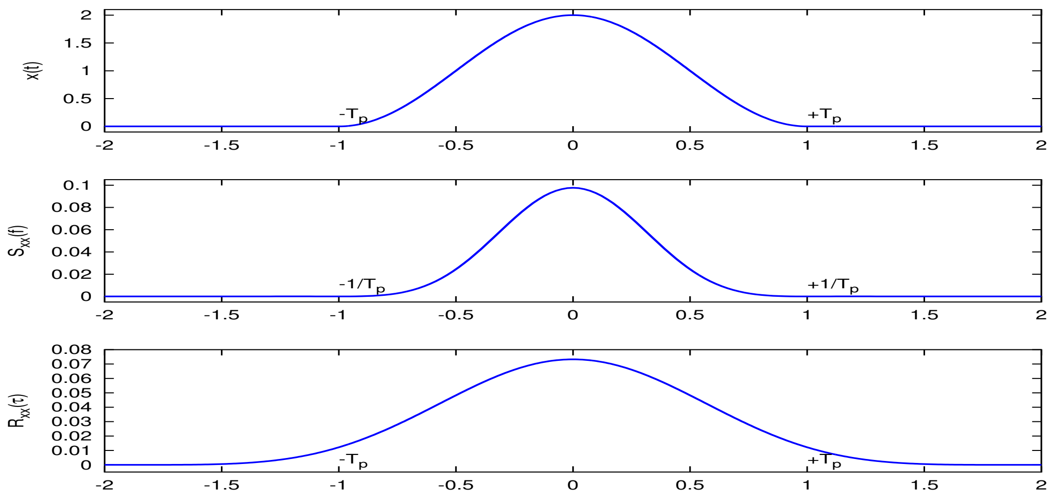
x(t)
-Tp
+Tp
Sxx(f)
-1/Tp
+1/Tp
Rxx(τ)
-Tp
+Tp

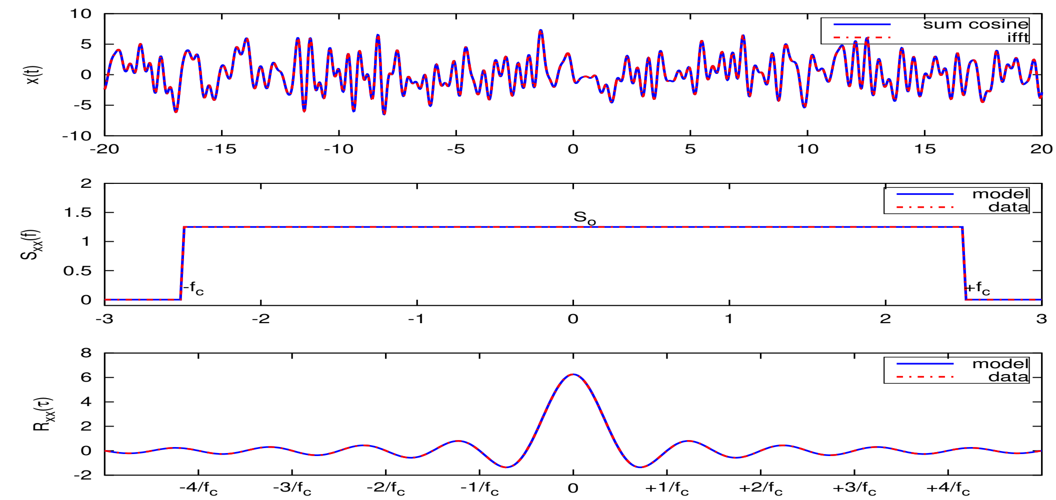
x(t)
sum cosine
ifft
Sxx(f)
model
data
So
-fc
+fc
Rxx(τ)
model
data
-4/fc
-3/fc
-2/fc
-1/fc
0
+1/fc
+2/fc
+3/fc
+4/fc

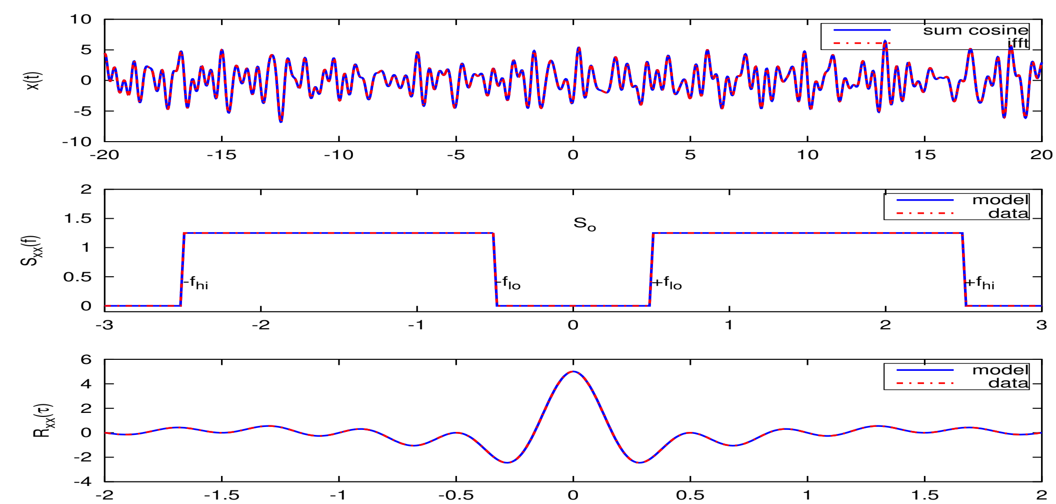
x(t)
sum cosine
ifft
Sxx(f)
model
data
So
-fhi
-flo
+flo
+fhi
Rxx(τ)
model
data

10 Power Spectral Densities for Natural Loads

10.1 Wind Turbulence

10.1.1 Davenport Wind Spectrum

The one-sided power spectral density of horizontal wind velocity, $u(t)$, may be modeled by the Davenport wind spectrum,

$$G_{UU}(f) = \sigma_U^2 \; \frac{2}{3} \; \frac{|fL/U_{10}|^2}{|f| \; (1 + |fL/U_{10}|^2)^{4/3}}$$

with model parameters:

- U_{10} = mean wind speed at 10 m elevation
- $\sigma_U^2 = 6kU_{10}^2$ = the mean square of the wind turbulence
- L = a turbulent length scale characteristic of upper atmosphere turbulence
- k = a dimensionless terrain roughness constant, (0.005 for open country, 0.05 for city)

The largest turbulence oscillations $fG_{UU}(f)$ occur at a frequency of $f_{\mathrm{p}} = \sqrt{3}\, U_{10}/L$.

This one-sided Davenport spectrum is scaled so that $\sigma_U^2 = \int_0^\infty G_{UU}(f) \; df$. Also, define $G_{UU}(0) = 0$.

10.1.2 Kaimal Wind Spectrum

The one-sided Kaimal wind turbulence spectrum has a power spectral density of

$$G_{UU}(f) = \sigma_U^2 \; \frac{4 \; (L/U)}{(1 + 6|f|(L/U))^{5/3}}$$

where

- U = the mean wind speed,
- $\sigma_U = T_i(3U/4 + 5.6)$, = the turbulence intensity,
- L = the Kaimal turbulence length scale, and reflects the size of wind eddies
- T_i = the turbulence intensity parameter (approx 0.2).

This one-sided Kaimal spectrum is scaled so that $\sigma_U^2 = \int_0^\infty G_{UU}(f) \; df$.

Referring to plots of the spectra on the next page, the Kaimal spectrum has a broader bandwidth than the Davenport spectrum. The (upper-atmosphere) Davenport turbulence length scale is about an order of magnitude larger than the Kaimal length scale for comparable spectra. At these length scales, most of the wind variability occurs at frequencies that are lower than the natural frequencies of structural systems (0.5 Hz to 5 Hz).

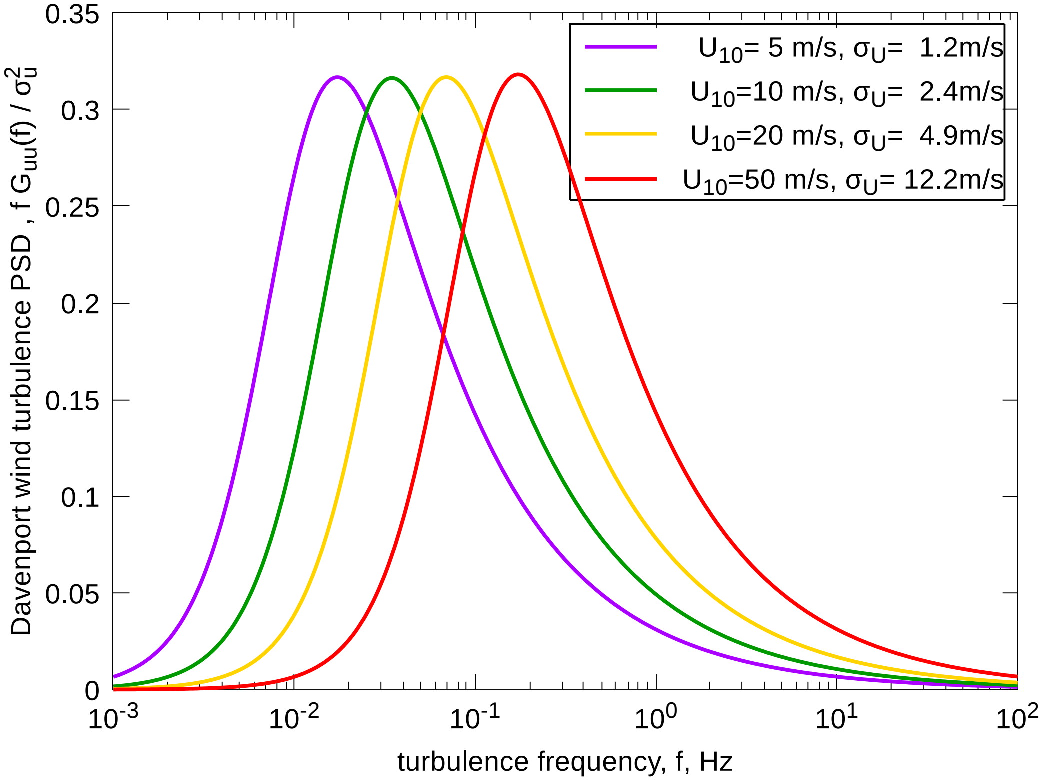

Figure 4. Davenport wind turbulence spectra with a Davenport length scale of $L = 500$ m and terrain roughness $k = 0.01$.

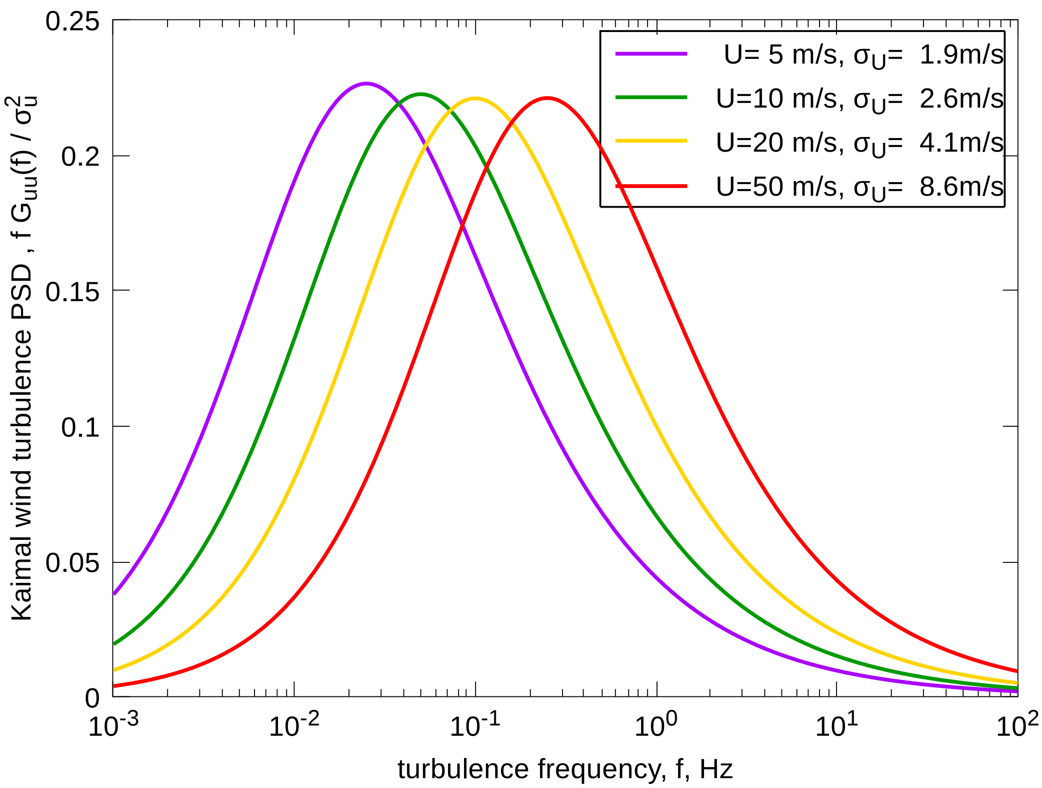

Figure 5. Kaimal wind turbulence spectra with a Kaimal length scale of $L = 50$ and a turbulence intensity $T_i = 0.2$.

10.2 Ocean Waves

10.2.1 Pierson-Moskowitz Spectrum

In a fully-developed sea with a uni-directional wave-field, the one-sided power spectral density of wave-height $z(t)$ can be modeled by the Pierson-Moskowitz spectrum,

$$G_{ZZ}(f) = \frac{\alpha g^2}{|2\pi f|^5} \exp\left[-\frac{5}{4}\left|\frac{f_\mathrm{p}}{f}\right|^4\right]$$

with model parameters:

- $\alpha =$ a dimensionless constant, 0.0081 for the North Atlantic
- $g =$ gravitational acceleration (9.81 m/s^2)
- $f_\mathrm{p} = g/[(1.14)(2\pi)U_{19.5}]$ is the frequency of the largest waves (Hz)
- $U_{19.5} =$ mean wind speed at 19.5 m above mean sea level ($U_{19.5} \approx (1.026)U_{10}$) (m/s)

and define $G_{ZZ}(0) = 0$. This spectrum is scaled so that the mean-square wave height is

$$\left\langle Z^2(t)\right\rangle = \sigma_Z^2 = 2\pi \int_0^\infty G_{ZZ}(f)\, df \approx \frac{\alpha}{g^2}\frac{U_{19.5}^4}{2.96}$$

So the standard deviation of the wave height is proportional to the mean wind speed squared, which is a strong-dependence on mean wind speed. The speed of the largest waves is

$$c_\mathrm{p} = \frac{g}{2\pi f_\mathrm{p}} \approx (1.14)U_{19.5}$$

The speed of the largest waves is 14% faster than the mean wind speed.

10.2.2 JONSWAP Spectrum

The Pierson-Moskowitz spectrum is a special case of the JONSWAP spectrum. The JONSWAP spectrum models developing seas and accounts for the distance from the shoreline (the “fetch”, F). through an additional factor, $\gamma^{\delta(f)}$.

$$G_{ZZ}(f) = \frac{\alpha g^2}{|2\pi f|^5} \exp\left[-\frac{5}{4}\left|\frac{f_\mathrm{p}}{f}\right|^4\right] \gamma^{\delta(f)}$$

where $G_{ZZ}(0) = 0$; γ is a magnification factor for the largest waves ($\gamma \approx 3.3$) and the exponent δ depends on frequency,

$$\delta(f) = \exp\left[-\frac{(1-|f/f_\mathrm{p}|)^2}{2(\sigma(f))^2}\right],$$

- $\alpha = 0.066\left(U_{10}^2/(gF)\right)^{0.22}$
- γ is the magnification of the largest waves $\ldots 1 < \gamma < 7 \ldots$ on average $\gamma \approx 3.3$.
- $f_\mathrm{p} = 2.84(g^2/(U_{10}F))^{0.33}$ is the frequency of the largest waves
- $\sigma(f) = 0.07$ for $|f| \le f_\mathrm{p}$, and $\sigma(f) = 0.09$ for $|f| > f_\mathrm{p}$
- psd scaling is: $\sigma_Z^2 = 2\pi \int_0^\infty G_{ZZ}(f)\, df$

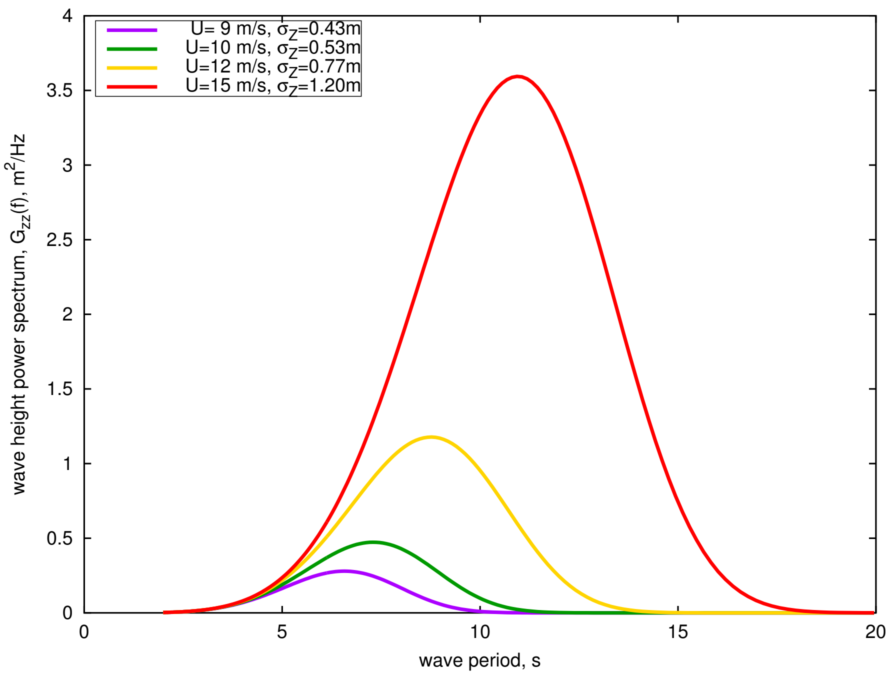

Figure 6. Pierson-Moskowitz spectra for fully-developed seas.

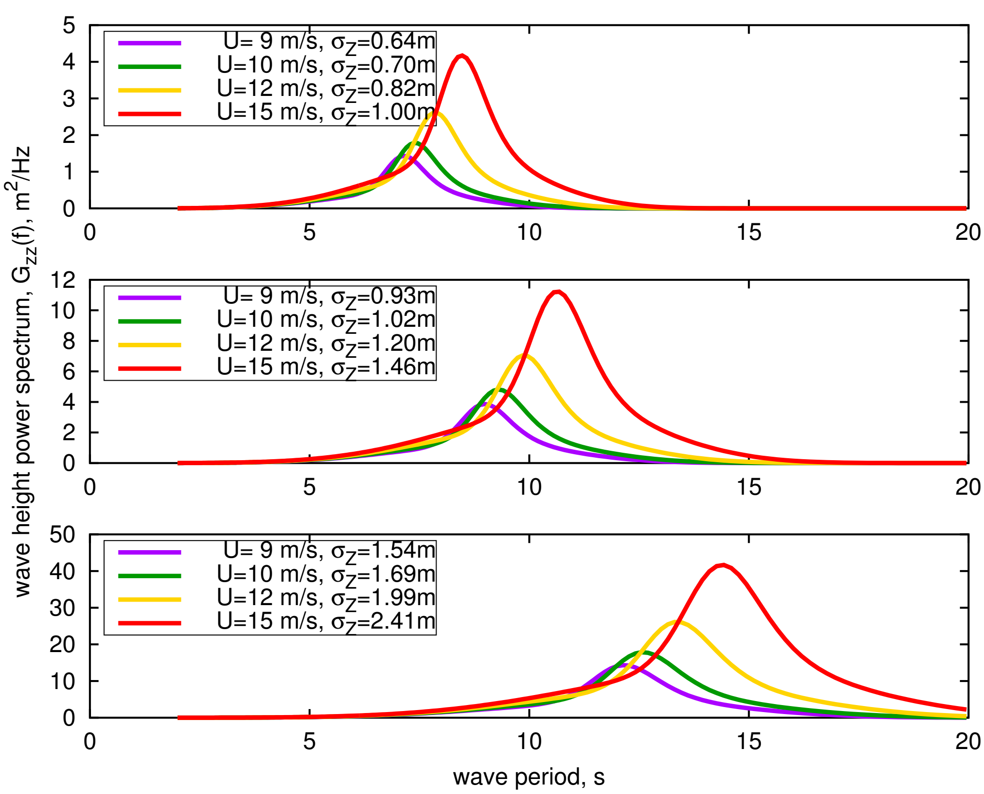

Figure 7. JONSWAP spectra with $\gamma = 3.3$ and F = 100 km, 200 km, and 500 km.

10.3 Earthquake Ground Motions

A one-sided power spectral density for ground accelerations,

$$G_{AA}(f) = \bar{a}^2 \; \frac{(2\zeta_g f/f_g)^2}{(1-(f/f_g)^2)^2 + (2\zeta_g f/f_g)^2}$$

is parameterized by:

- f_g, a ground motion frequency (Hz) and
- ζ_g, a ground motion damping ratio.

This spectrum corresponds to a linear time-invariant system with a realization

$$\left[\begin{array}{c|c} A & B \\ \hline C & D \end{array}\right] \sim \left[\begin{array}{cc|c} 0 & 1 & 0 \\ -4\pi^2 f_g^2 & -4\pi\zeta_g f_g & \bar{a} \\ \hline 0 & 4\pi\zeta_g f_g & 0 \end{array}\right]$$

The mean-square value of the ground accelerations is

$$\left\langle A^2(t) \right\rangle = \sigma_A^2 = \int_0^\infty G_{AA}(f)\; df = \pi\; \bar{a}^2\; f_g z_g$$

However, unlike the models for wind turbulence and ocean waves described in the previous sections, earthquake ground motions have time-varying amplitudes. An *envelope function* that mimics the growth and decay of earthquake ground motions is

$$e(t) = (ab)^{-a}\; t^a\; \exp(a - t/b)$$

which has a maximum of $e(t)$ is 1 and occurs at time $t = ab$.

The spectral and temporal characteristics of earthquake ground motion are influenced by many factors, primarily the magnitude of the rupture, the distance to the fault, the depth of the rupture, and the local soil conditions. Strong ground motions at sites far from a fault tend to have higher frequency content and longer duration. Ground motions at sites close to a fault can have a large amplitude pulse, depending on the directivity of the fault rupture in relation to the site and other factors.

Relevant models for earthquake ground motions generate the kinds of structural responses excited by real (recorded) ground motions. For this reason, the model parameters $\bar{a}$, f_g, ζ_g, a, and b are adjusted so that, on average, the mean response spectra of the synthetic ground motions match the response spectra from representative sets of earthquake ground motions. This fitting was carried out with three suites of recorded ground motions for the ATC-63 project on structural collapse, with the resulting response spectra and model parameters shown below.

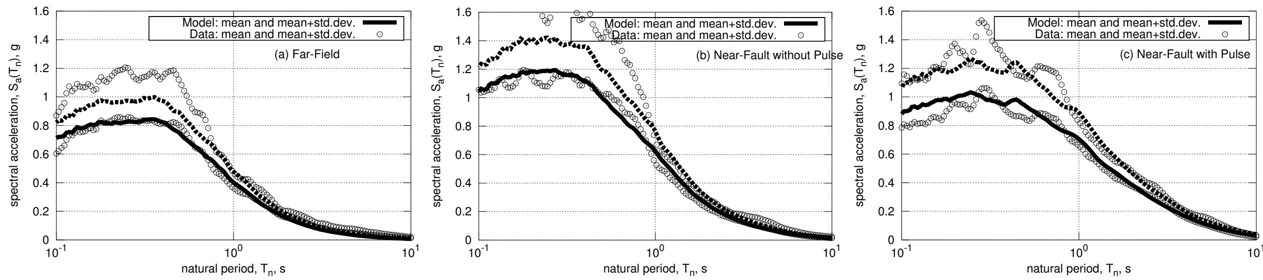

Table 3. Ground motion parameters fit to the ATC-63 ground motion suites.

	PGV	f_g	z_g	a	b	$\bar{a}$
FF	0.33	1.5	0.9	4.0	2.0	0.23
NF-NP	0.52	1.3	1.1	3.0	2.0	0.33
NF-P	0.80	0.5	1.8	1.0	2.0	0.43
	m/s	Hz	-	-	s	m/s^2

Either of the two amplitude constants PGV (peak ground velocity) or $\bar{a}$ may be used to specify the amplitude of the ground motion. If PGV is used the ground motion is scaled to the specified peak value.

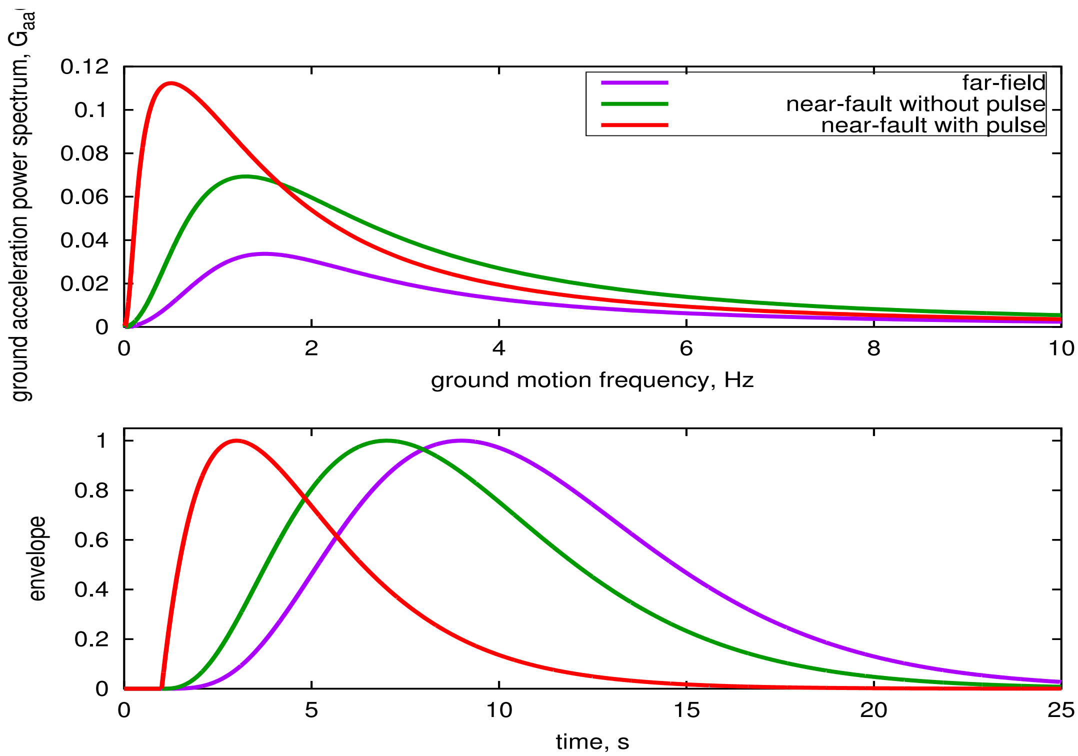

Figure 8. Spectra and envelopes for three classes of earthquake ground motions.

Synthesized ground motion accelerations may be detrended so that the ground velocity is zero and the ground displacement is nearly zero at the end of the synthesized ground motion, as illustrated by the example realizations on the next page.

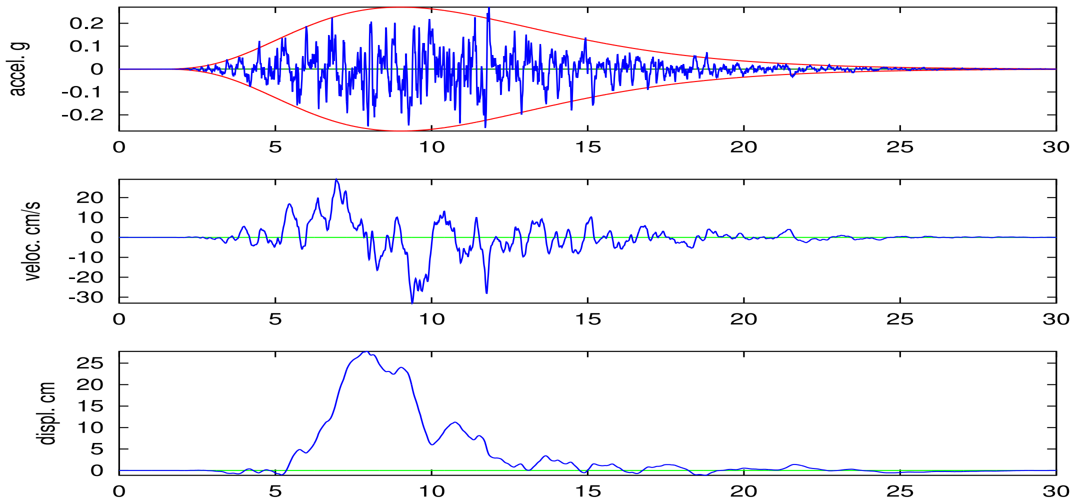
accel. g
veloc. cm/s
displ. cm
0 5 10 15 20 25 30

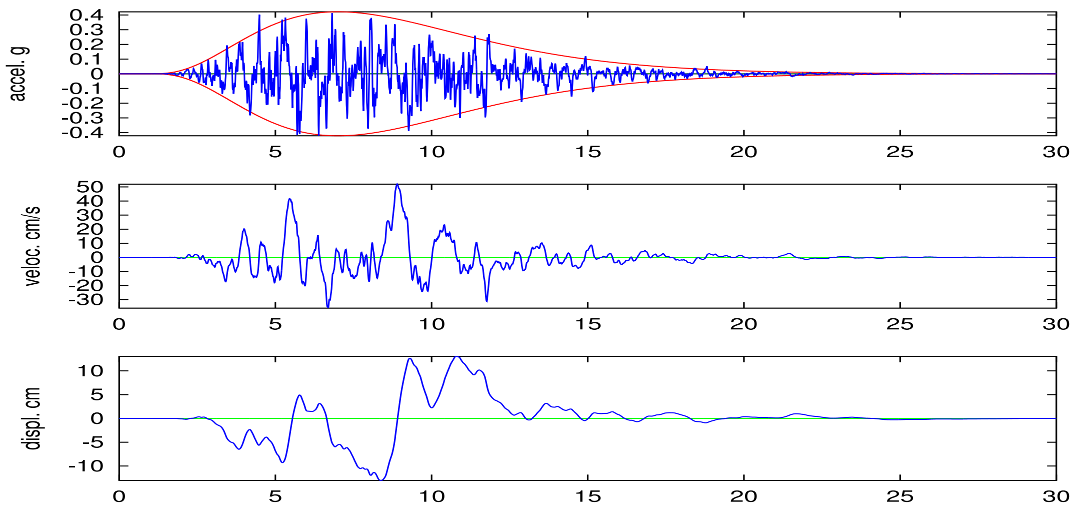
accel. g
veloc. cm/s
displ. cm
0 5 10 15 20 25 30

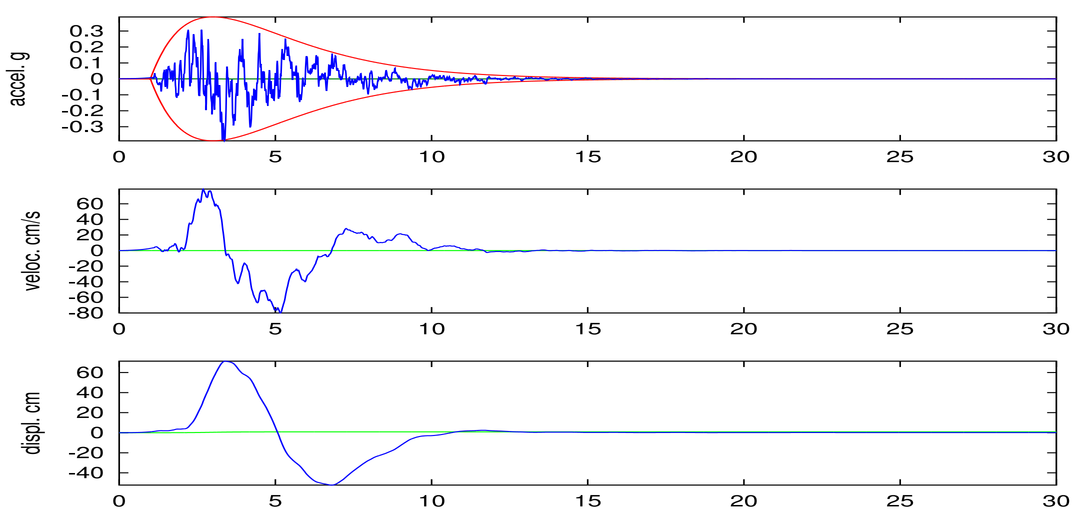
accel. g
veloc. cm/s
displ. cm
0 5 10 15 20 25 30

11 Finite-time discrete unit Gaussian white noise

A finite-length time series of unit Gaussian white noise is a series of samples from a set of n independent identically-distributed (iid) Gaussian random variables,

$$u = \left[\begin{array}{ccccccc} u_0 & u_1 & u_2 & \cdots & u_p & \cdots & u_{n-1} \end{array} \right]$$

with zero mean and a variance of $1/(\Delta t)$, where (Δt) is the sampling interval.

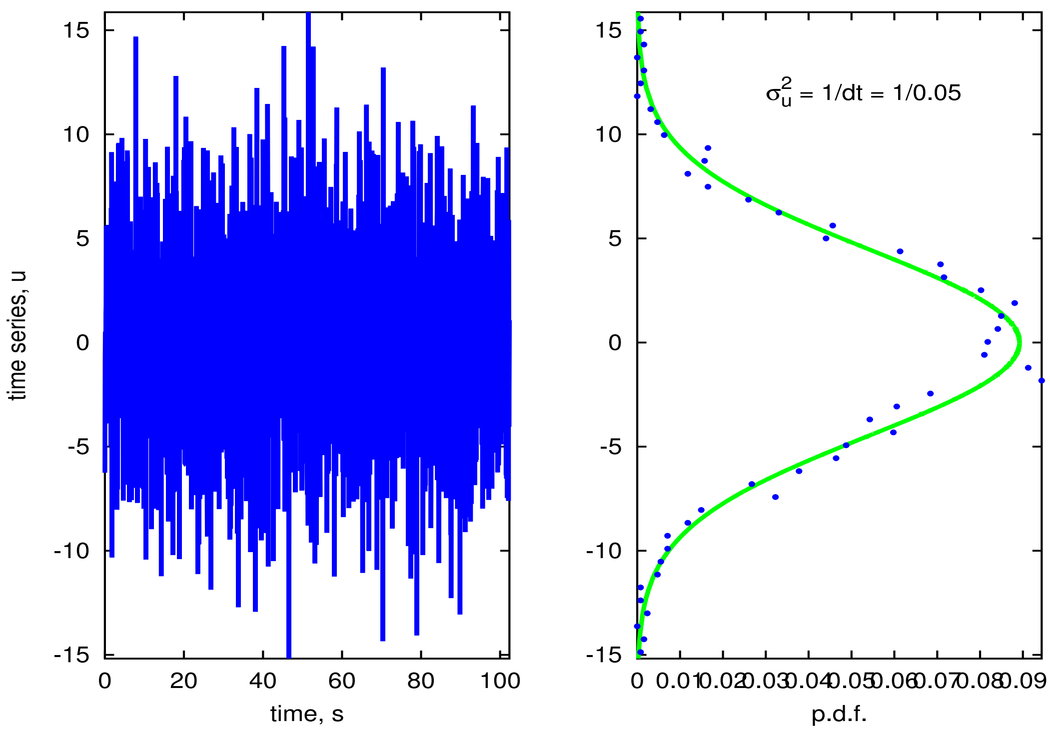

Figure 9. Gaussian unit white noise with $(\Delta t) = 0.05$ s, $n = 2048$; computed with `u=randn(1,n)/sqrt(dt);` $T = (n)(\Delta t) = 102.4$ s and $\sigma_u = \sqrt{1/(\Delta t)}$. points: histogram of sample, line: Normal distribution

The complex Fourier coefficients $\bar{U}_q$ for this series can be computed with a discrete Fourier transform,

$$\bar{U}_q = \frac{1}{n} \sum_{p=0}^{n-1} u_p \, \exp\left(-i \frac{2\pi qp}{n}\right) \, , \quad q = \left[\, -\tfrac{n}{2}+1, \quad -\tfrac{n}{2}+2, \quad \cdots , \quad -1, \quad 0, \quad 1, \quad \cdots . \quad \tfrac{n}{2} \, \right]$$

where u_p is $(p+1)^{\text{st}}$ element of the sequence of uncorrelated standard Gaussian random variables. So, $\bar{U}_q$ is a weighted sum of Gaussian random variables, where the weights

$$e^{-i2\pi qp/n} = \cos(2\pi qp/n) + i \sin(2\pi qp/n)$$

are complex-valued. The frequency increment (Δf) equals $1/T$, and the Nyquist frequency range is $-1/(2\Delta t) < f \leq 1/(2\Delta t)$.

If the input to a dynamical system is discrete unit Gaussian white noise, then the power spectral density of the output of the system is equal to the magnitude-squared of the system frequency response function. This is a common application of Gaussian white noise in the context of dynamic systems analysis. It is therefore helpful to understand the statistical properties of unit Gaussian white noise.

Finite time discrete unit Gaussian white noise has the following provable properties:

- The real parts of the Fourier coefficients $\bar{U}_q$ are symmetric about $q = 0$ (even); the odd parts of $\bar{U}_q$ are anti-symmetric about $q = 0$ (odd). Both the real and imaginary parts of $\bar{U}_q$ have zero mean, and a variance of $1/(2T)$ (figure 10).
- The real and imaginary parts of U_q are uncorrelated (figure 11).
- The Fourier magnitudes, $|\bar{U}_q|$, have a Rayleigh distribution with parameter $\sigma = \sqrt{1/(2T)}$ and the Fourier phase, $\arctan(\mathbb{I}(\bar{U}_q)/\mathbb{R}(\bar{U}_q))$, is uniformly distributed in $[-\pi : \pi]$ (figure 12).
- The auto-power spectral density of sampled unit white noise has an expected value of 1 over the Nyquist frequency range. The auto-power spectral density is a χ^2-distributed random variable with a degree-of-freedom (d.o.f.) of 2, and a variance of 1. The coefficient of variation of the power spectral density of unit Gaussian white noise is therefore also 1 (figure 13).
- The auto-correlation $R(\tau)$ of sampled unit white noise resembles $\delta(\tau)$ with $R(0) = \sigma_u^2 = 1/(\Delta t)$ (figure 14).
- The fact that the power spectral density estimate from a sample of Gaussian white noise has a coefficient of variation of 1 means that the uncertainty in the PSD estimate is as large as the mean PSD value. This presents a challenge in the estimation of PSD's from noisy data. This coefficient of variation can be reduced by averaging PSD's together.

  The average of K PSD's of independent samples of unit Gaussian white noise is a χ^2-distributed random variable with $2K$ degrees of freedom, a covariance of $1/K$ and a coefficient of variation of $\sqrt{1/K}$ (figure 15).

Note that the generation of a random time series from a given power spectral density function (as in example 2 of section 8) results in a time series with *exactly* the prescribed power spectral density. If the generated time series is meant to represent a random phenomenon, then it would be appropriate to randomize the Fourier amplitudes with a Rayleigh distribution.

The reduction of the variance of PSD estimates with averaging motivates the Welch method for estimating power spectral densities from measurements of noisy time series.

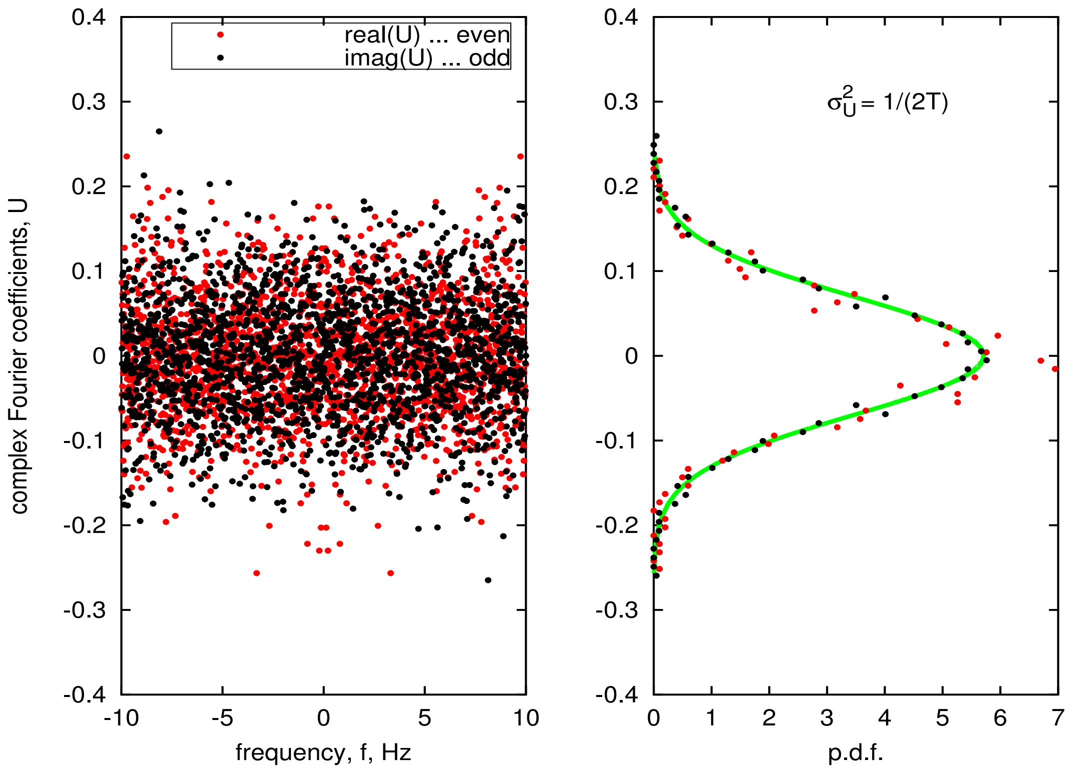

Figure 10. Fourier transform coefficients of the sample of Gaussian unit white noise shown in figure 9. computed with `U=fft(u)/n;` points: histogram of sample, line: Normal distribution

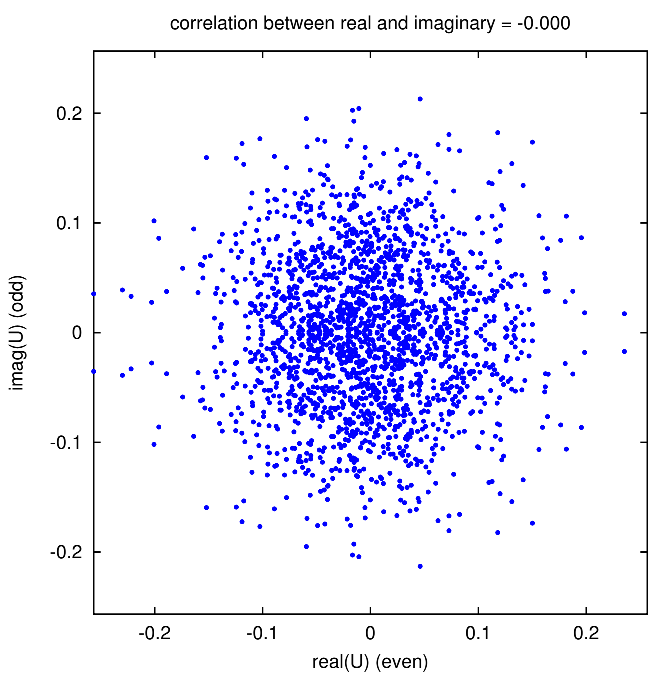

Figure 11. The real and imaginary parts of U_q are uncorrelated.

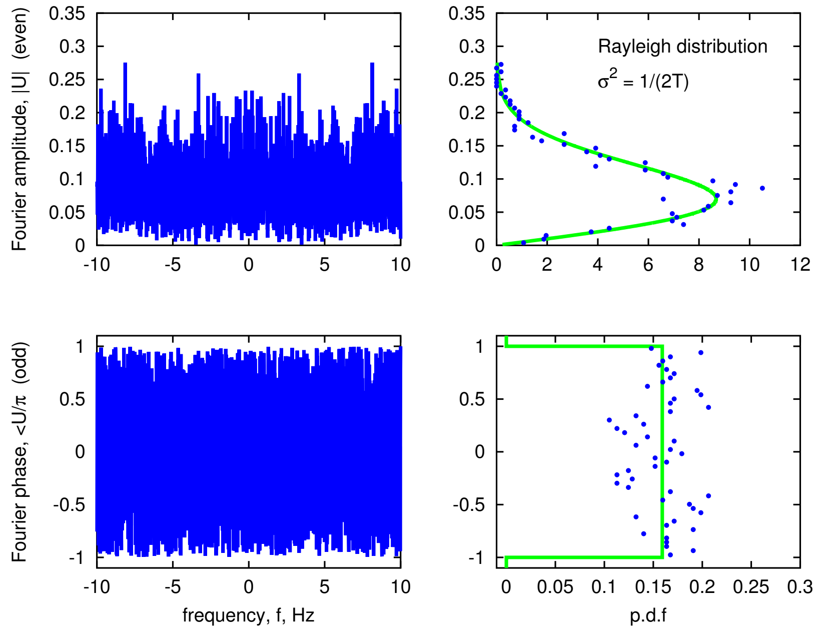

Figure 12. Fourier transform magnitudes and phases of the sample of Gaussian unit white noise shown in figure 9, The magnitudes are symmetric about $f = 0$ (even); the phases are anti-symmetric about $f = 0$ (odd). points: histogram of sample, line: Rayleigh distribution for $|U|$ and uniform distribution for $\angle U$

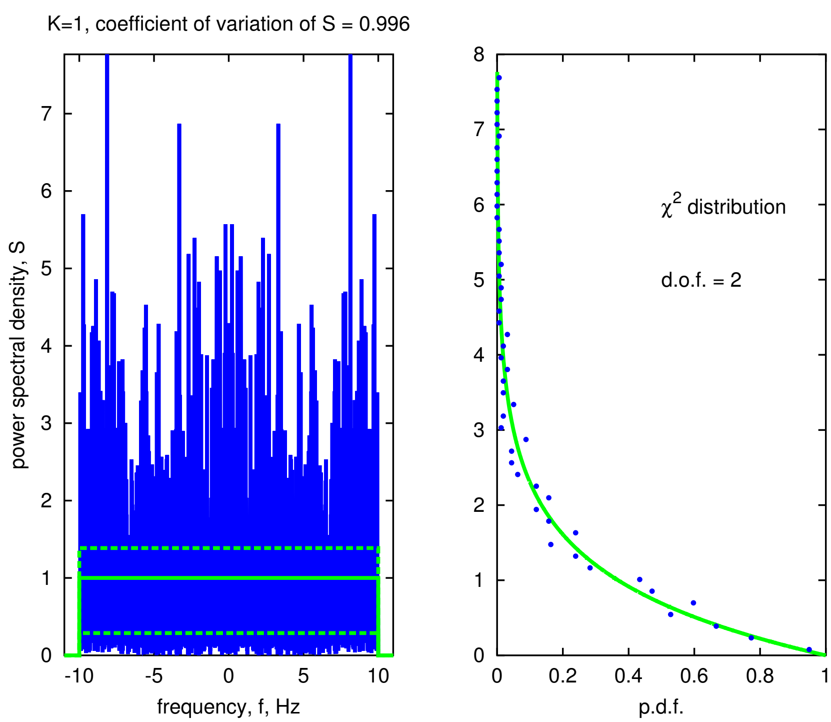

Figure 13. Power spectral density of the sample of unit Gaussian noise shown in figure 9. computed with `S=conj(U)*U/(df)` Dashed lines show the 50% confidence interval for the power spectral density. left: points = histogram of the PSD data, line = χ^2 distribution

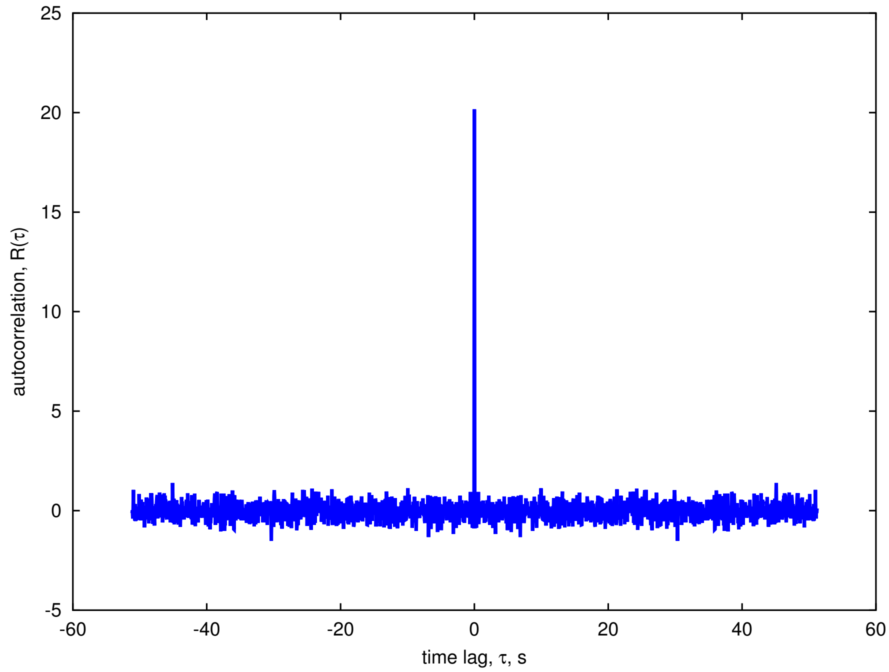

Figure 14. Auto-correlation function of the sample of unit Gaussian noise shown in figure 9. computed with `R=ifft(S)/df`

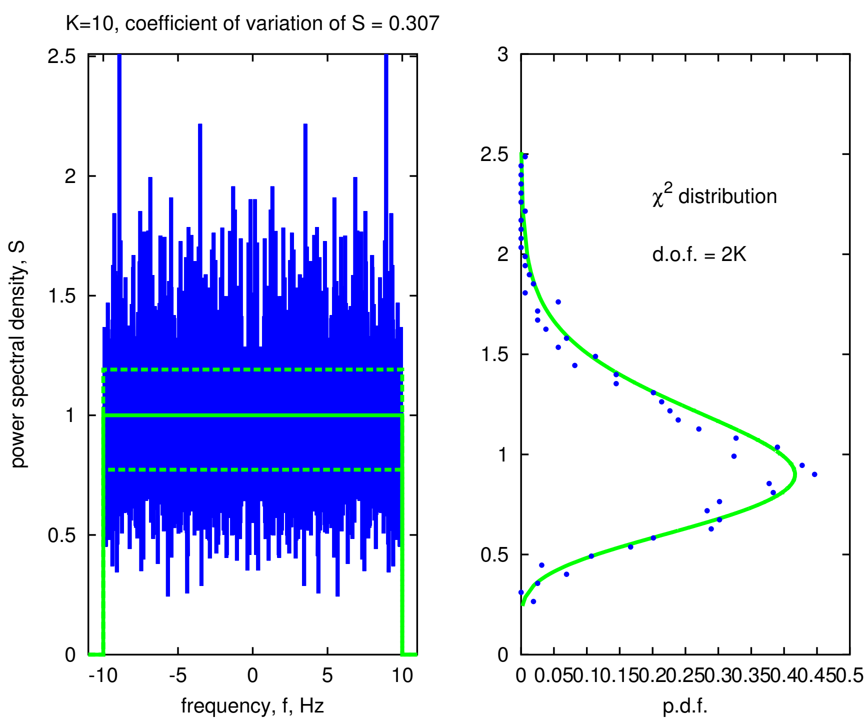

Figure 15. Average of power spectral densities from $K = 10$ independent samples of unit Gaussian white noise. Dashed lines show the 50% confidence interval for the power spectral density. left: points = histogram of the PSD data, line = χ^2 distribution with $2K$ degrees of freedom.

12 Estimating power spectral density from noisy data via FFT: psd.m

The previous section, and Figures 9 and 15 show that averaging the magnitude-square of the Fourier amplitudes computed from several independent realizations of the same (stationary) random process reduces the variance of the power spectral density estimate.

Fourier analysis of any finite-duration time series fundamentally presumes that the series repeats periodically. If the series is representative of a discrete-time random process then a sub-sequence of n points from the process does not repeat itself periodically; $x_k \neq x_{k+n} \forall k, 1 \leq k \leq n$. Furthermore, the periodic extension of a non-periodic n-point segment contains a sharp discontinuity between x_1 and x_n. The Fourier components of sequences with sharp discontinuities *do not* approach zero as the frequency approaches the Nyquist frequency. In fact, these high-frequency spectral magnitudes can be quite a bit larger than those of the true band limited process.

Welch's method estimates the power spectral density of a discrete-time sequence by averaging the FFT amplitudes of windowed sub-sequences. The steps of the algorithm are as follows:

1. Extract K sub-sequences of n points from a long time series (of N points). If the n-point sub-sequences overlap by n_o points, $K = \lfloor (N - n_o)/(n - n_o) \rfloor$. For greatest numerical efficiency, n should be a power of 2. To minimize the variance of the PSD estimate from a record of pre-measured time-series, set $n_o = n/2$, which gives $K = 2N/n - 1$, and a reduction in variance by a factor of approximately $9K/11$ [2] . See Figure 17.

2. Detrend each sub-sequence, either by subtracting the mean of the sub-sequence, or by subtracting the least-squares best-fit straight line through the sub-sequence.

3. Multiply each sub-sequence by a real-valued window sequence w_k, $(k = 1, ..., n)$, that tapers the amplitude to zero at both ends ([10] section 13.4).

   Common window choices are:

square:	$w_k = 1$
Welch:	$w_k = 1 - (2k/n - 1)^2$
sine:	$w_k = \sin(\pi(k - 1/2)/n)$
Lanczos:	$w_k = \mathrm{sinc}(2(k - 1)/(n - 1) - 1)$
Hamming:	$w_k = 0.53836 - 0.46146 \cos(2\pi k/n)$
Gauss:	$w_k = \exp(-(1/2)((k - n/2)/(n/5))^2)$
Hanning:	$w_k = (1 + \cos(2\pi(k - n/2)/n))/2$
Bartlett:	$w_k = 1 - \lvert 2k/n - 1 \rvert$

   These functions, and their spectral shapes, are plotted in Figure 16.

   The choice of the window function affects the width of spectral peaks, and the degree to which spectral content that is not exactly matched to a Fourier frequency "leaks" into adjacent frequency bins. If the signal is known to contain frequencies *only* at the Fourier frequencies, then a square window will give the narrowest peaks, and the spectral leakage from other (Fourier) frequencies will be precisely zero. This is almost never the case. (The signal is almost surely to contain spectral content at frequencies between the Fourier frequencies.) Windowing the data prior to computing the FFT narrows the peaks associated with a non-Fourier frequency component, and suppresses the leakage of signal energy throughout the spectrum. So, the choice of window function controls the trade-off between narrow peaks and leakage into adjacent frequency bins.

Of the window functions illustrated here and excluding the square window, the Gauss window has the widest peak but the least amount of leakage into adjacent frequencies, whereas the Welch window has the most narrow peak, but with more leakage into adjacent frequencies.

4. Compute the average of the FFT magnitudes of each windowed sub-sequence. Y

5. Compute the power spectral density by multiplying the averaged FFT magnitudes by the time step, Δt, and dividing by square of the norm of the window function, $||w||^2$. In this way the two-sided PSD agrees with Parseval's theorem.

6. Confidence intervals for the PSD estimation may optionally be computed via the χ^2 inverse CDF with $(2K)(9K/11)$ degrees of freedom,

$$S_{XX}(f)(\chi^2)^{-1}(\alpha/2,(2K)(9K/11))/((2K)(9K/11)) \leq S_{XX}(f)$$

$$S_{XX}(f) \leq S_{XX}(f)(\chi^2)^{-1}(1-\alpha/2,(2K)(9K/11))/((2K)(9K/11))$$

where $(1-\alpha)$ is the confidence level.

As an example of the Welch method to compute the PSD, we compute the PSD from a record corresponding to the model power spectral density function:

$$S_{XX}(f) = \frac{10^{-6}}{(((f/10)^2-1)^2+10^{-3}(f/10)^2)^2} + \frac{1}{(1+(f/10)^2)^2}$$

In these calculations, $\Delta t = 0.01$s; $N = 4096$, and $n = 512$ or 1024. The time-series sample is computed from the power spectral density via the IFFT and uniformly-distributed phases.

```
theta = 2*pi*rand(1,N/2) - pi;                  % uniformly-distributed phases
theta = [ 0 , theta , -theta(N/2-1:-1:1) ];     % phase angles anti-symmetric about f=0
theta(N/2+1) = 0;                               % for real-valued signals
x = real(ifft(sqrt(Sxx*df) .* exp(i*theta)))*N; % imag part ~ 1e-16
```

Power spectral densities are then computed from the time-series using 7 windows of $n = 1024$ points and 15 windows of $n = 512$ points. The results are shown in Figure 18.

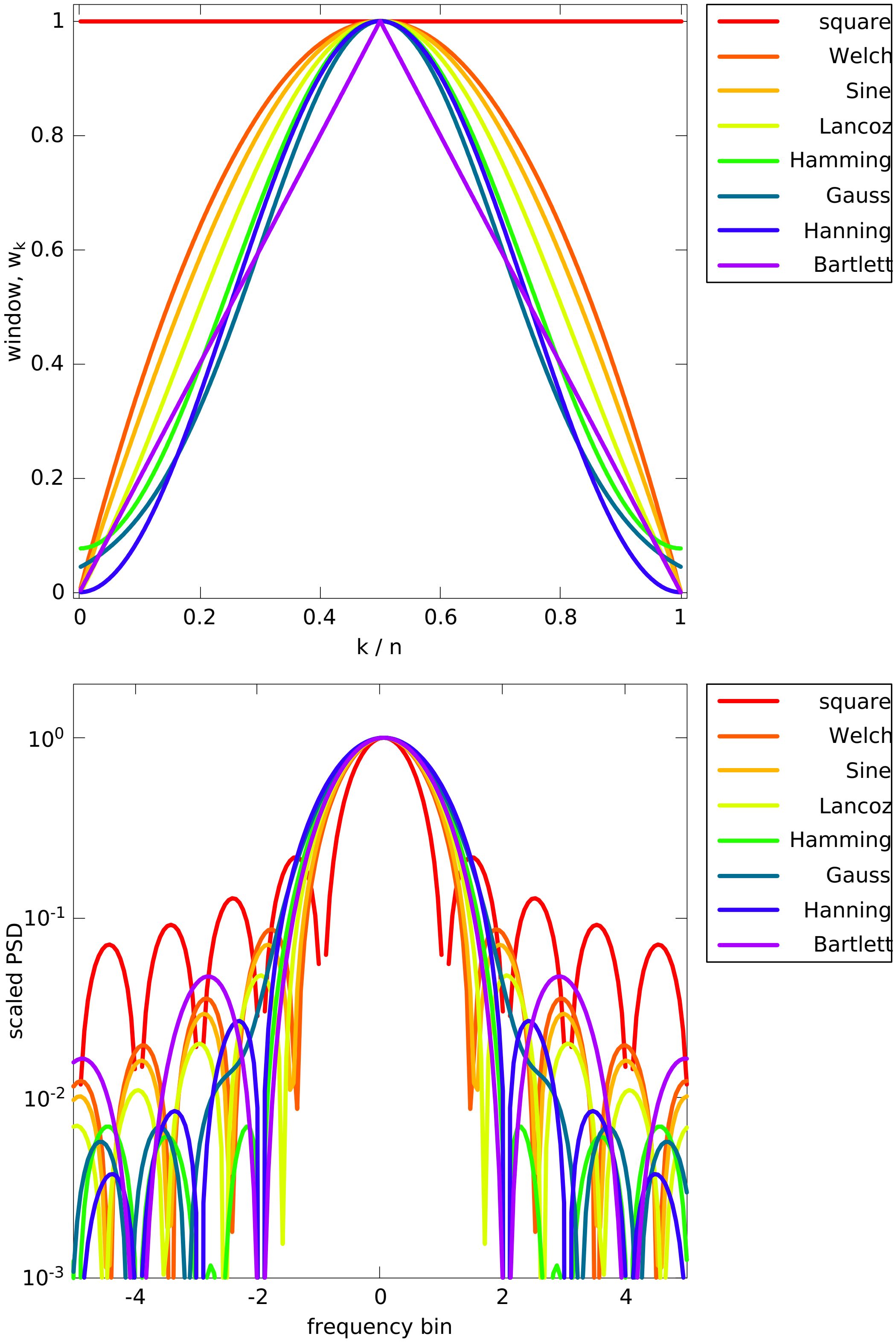

Figure 16. Window functions for PSD computations and their associated spectral shapes

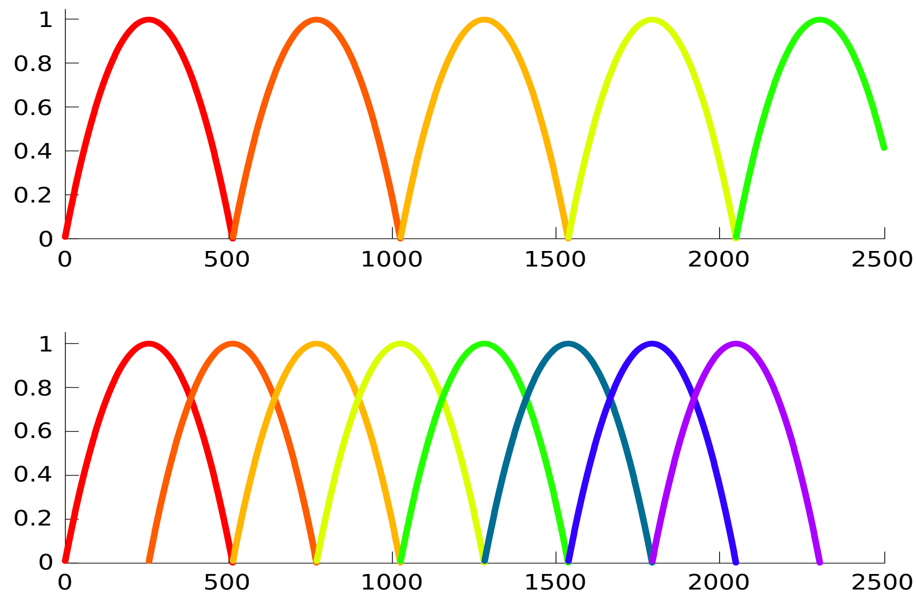

Figure 17. non-overlapping Welch windows and 50% overlapping Welch windows

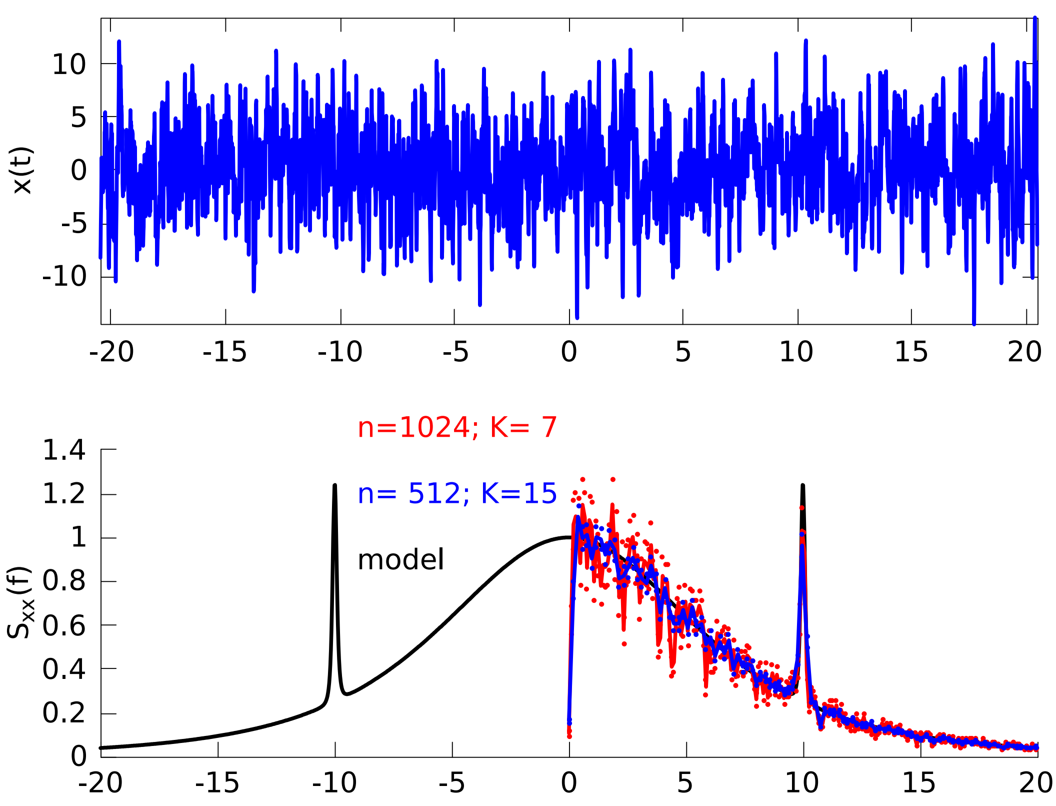

Figure 18. A random sequence corresponding to a particular power spectral density, and the power-spectral density estimated via the Welch method. solid lines: PSD computed, dots: 50% confidence interval

13 Estimating frequency response functions from noisy data via FFT: tfe.m

In the frequency-domain, the relationship between the true inputs u and true outputs y is the frequency-response function $H_o(f)$. The frequency response function may be easily estimated from the Fourier transforms of the true inputs $\bar{Y}(f)$ and outputs $\bar{U}(f)$.

$$\bar{Y}(f) = H_o(f)\ \bar{U}(f) \qquad \Leftrightarrow \qquad H_o(f) = \frac{\bar{Y}(f)}{\bar{U}(f)}$$

In the absence of measurement noise, the frequency response function may be computed from either of the ratios of Fourier transforms below.

$$H_o(f) = \frac{\bar{Y}^*(f)\bar{Y}(f)}{\bar{Y}^*(f)\bar{U}(f)} = \frac{\bar{U}^*(f)\bar{Y}(f)}{\bar{U}^*(f)\bar{U}(f)}$$

However, measurements of the input and output $\hat{u}$ and $\hat{y}$ typically contain random measurement noise, n and m. (See Figure 19.) As described in section 10, noise in a finite-time discrete random process propagates directly to randomness in the Fourier coefficients. So an estimate of a frequency response function obtained by a ratio of noise-corrupted Fourier transforms would also contain significant noise. Fortunately, noise in power spectral density estimates of noisy data can be reduced, through a process of windowing and averaging, as described in section 11. From section 5, the cross-power spectral density

$$S_{YU} = \lim_{T\to\infty} \mathbb{E}\left[\frac{1}{T}\bar{Y}^*(f)\ \bar{U}(f)\right] = \int_{-\infty}^{\infty} R_{YU}(\tau)e^{-\mathrm{i}2\pi f\tau}d\tau$$

Assuming the noise processes n and m are uncorrelated with each other and with the true input and the true output, the associated cross-power spectra are all zero:

$$S_{NM}(f) = 0; \quad S_{MU}(f) = 0; \quad S_{MY}(f) = 0; \quad S_{NU}(f) = 0; \quad S_{NY}(f) = 0.$$

With this assumption, it is not hard to show that

$$S_{\hat{U}\hat{U}}(f) = S_{UU}(f) + S_{NN}(f); \qquad S_{\hat{Y}\hat{Y}}(f) = S_{YY}(f) + S_{MM}(f); \qquad S_{\hat{Y}\hat{U}}(f) = S_{YU}(f)$$

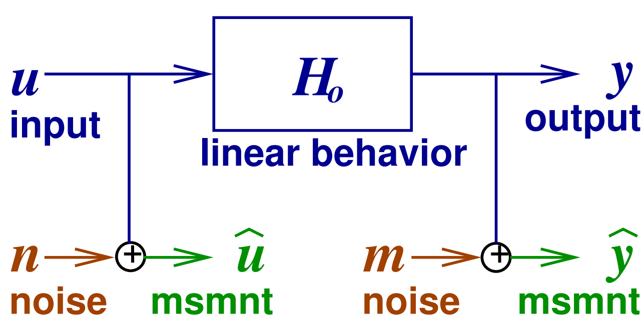

Figure 19. A block diagram of a linear system with noisy measurements.

With these assumptions on the noise processes, we can use power spectral density estimates to compute lower and upper bounds $H_1(f)$ and $H_2(f)$ on the true frequency response function $H_o(f)$.

$$H_1(f) = \frac{S_{\hat{Y}\hat{U}}(f)}{S_{\hat{Y}\hat{Y}}(f)} = \frac{S_{YU}(f)}{S_{YY}(f) + S_{MM}(f)} < H_o(f)$$

$$H_2(f) = \frac{S_{\hat{U}\hat{U}}(f)}{S_{\hat{U}\hat{Y}}(f)} = \frac{S_{UU}(f) + S_{NN}(f)}{S_{UY}(f)} > H_o(f)$$

An estimate of the frequency response function that simultaneously minimizes the effects of the input measurement noise and the output measurement noise is the geometric mean of the bounds [11].

$$H_v(f) = \sqrt{H_1(f)\ H_2(f)}$$

The ratio of these bounds is called the *coherence* function.

$$\gamma^2(f) = \frac{H_1(f)}{H_2(f)} = \frac{|S_{YU}(f)|^2}{S_{XX}(f) S_{YY}(f)} \qquad 0 \le \gamma^2 \le 1$$

The coherence function indicates the frequency-dependence of the amount of measured response that can be linearly related to the measured input. At any given frequency, the coherence is less than unity if

- there is significant noise on the input or the output,
- the output is driven by unmeasured inputs, or
- the output is nonlinearly related to the input.

14 Response Statistics of Linear Systems Driven by Uncorrelated White Noise

Recall the modeling of linear time-invariant multi-input, multi-output (MIMO) systems:

$$\dot{x}(t) = Ax(t) + Bu(t)$$

$$y(t) = Cx(t) + Du(t)$$
$$H(\omega) = C(i\omega I - A)^{-1}B + D$$
$$H(t) = Ce^{At}B$$

Given a system model (A, B, C, D) and the power spectral density of a stationary input process $S_{UU}(f)$, the power spectral density of the output process $S_{YY}(f)$ is

$$S_{YY}(f) = |H(f)|^2 \; S_{UU}(f)$$

from which,

$$\left\langle y^2(t) \right\rangle = \int_{-\infty}^{\infty} S_{YY}(f) \; df$$

As an example, for a scalar second-order system

$$\ddot{r} + 2\zeta\omega_{\mathrm{n}}\dot{r} + {\omega_{\mathrm{n}}}^2 r = u(t)$$

$$|H(f)|^2 = \frac{(f/f_n)^4}{\left(1 - (f/f_n)^2\right)^2 + (2\zeta f/f_n)^2}$$

If the system is lightly damped ($\zeta < 0.1$), and $S_{UU}(f_n)$ is roughly constant over the resonant bandwidth, then the random process y is dominated by frequencies near resonance, and

$$\left\langle r^2(t) \right\rangle \approx f_n \; \frac{\pi}{4\zeta} \; S_{UU}(f_n) \; .$$

More generally, if the input process is uncorrelated unit white noise, then

$$\left\langle y^2(t) \right\rangle = \mathrm{diag}(CQC^{\mathsf{T}})$$

where Q is the steady-state state covariance matrix $Q = \lim_{t\to\infty} \mathsf{E}[x(t)x^{\mathsf{T}}(t)]$ and solves the Liapunov equation

$$0 = AQ + QA^{\mathsf{T}} + BB^{\mathsf{T}} = 0 \; .$$

If the input process U is uncorrelated unit white Gaussean noise, then the output process is also Gaussean. So, with $\sigma_y^2 \equiv \langle y^2(t) \rangle$ (and $\mu_y = 0$),

$$\mathrm{Prob}[Y > \hat{y} \; \cap \; Y < -\hat{y}] = 2\Phi(-\hat{y}/\sigma_y)$$

where $\Phi(z)$ is the standard normal cumulative distribution function.

Note that any spectral moment λ_m may be calculated from the solution of an approriately defined Liapunov equation.

15 Extremes of Random Processes

Consider the probability of an upcrossing through a positive-valued threshold, $\hat{y}$,

$$\text{Prob}[Y(t) < \hat{y} \cap Y(t+dt) > \hat{y}] \approx \text{Prob}[Y(t) < \hat{y} \cap Y(t) + \dot{Y}(t)dt > \hat{y}]$$

which is equivalent to

$$\text{Prob}[Y(t) < \hat{y} \cap Y(t) > \hat{y} - \dot{Y}(t)dt] \approx \int_0^\infty f_{Y,\dot{Y}}(\hat{y}, \dot{y}) \; |\dot{y} \; dt| \; d\dot{y} = \nu_{\hat{y}} \; dt$$

where $f_{Y,\dot{Y}}(y, \dot{y})$ is the joint probability distribution between the process Y and its derivitive $\dot{Y}$. The expression above defines the mean upcrossing rate $\nu_{\hat{y}}$

$$\nu_{\hat{y}} = \int_0^\infty f_{Y,\dot{Y}}(\hat{y}, \dot{y}) |\dot{y}| \; d\dot{y}$$

The mean number of upcrossings through a threshold $\hat{y}$ over a time interval T is $\nu_{\hat{y}} T$. The cross-correlation between Y and $\dot{Y}$ is $R_{Y,\dot{Y}}(\tau = 0)$. Recall that

$$R_{Y,\dot{Y}} = \frac{d}{d\tau} R_{Y,Y}(\tau)$$

and that at $\tau = 0$, the autocorrleation is maximum, so, $R_{Y,\dot{Y}}(\tau = 0) = 0$, the process Y and its derivitive $\dot{Y}$ are independent, and the joint distribution $f_{Y,\dot{Y}}$ is the product of the marginals, $f_{Y,\dot{Y}}(y, \dot{y}) = f_Y(y) f_{\dot{Y}}(\dot{y})$.

More specifically, if Y is Gaussean, the process $\dot{Y}$ is also Gaussean,

$$f_Y(y) = \frac{1}{\sqrt{2\pi}\sigma_y} \exp\left[-\frac{1}{2}(y/\sigma_y)^2\right]$$

$$f_{\dot{Y}}(\dot{y}) = \frac{1}{\sqrt{2\pi}\sigma_{\dot{y}}} \exp\left[-\frac{1}{2}(\dot{y}/\sigma_{\dot{y}})^2\right]$$

so Y and $\dot{Y}$ are independent and jointly Gaussean, $f_{Y,\dot{Y}}(y, \dot{y}) = f_Y(y) f_{\dot{Y}}(\dot{y})$, and the mean upcrossing rate is

$$\nu_{\hat{y}} = \int_0^\infty \frac{1}{2\pi} \frac{1}{\sigma_y} e^{-\frac{1}{2}(\hat{y}/\sigma_y)^2} \frac{1}{\sigma_{\dot{y}}} e^{-\frac{1}{2}(\dot{y}/\sigma_{\dot{y}})^2} \dot{y} \; d\dot{y}$$

Note that only the second exponential depends on $\dot{y}$, the variable of integration. So the first exponential may be moved outside of the integral. Now with a change of variables, $u = \dot{y}/\sigma_{\dot{y}}$ and $z = \frac{1}{2}u^2$, $d\dot{y} = \sigma_{\dot{y}} du$ and $dz = u \; du$.

$$\int_0^\infty \frac{\dot{y}}{\sigma_{\dot{y}}} e^{-\frac{1}{2}(\dot{y}/\sigma_{\dot{y}})^2} \; d\dot{y} = \int_0^\infty u \; e^{-\frac{1}{2}u^2} \sigma_{\dot{y}} \; du = \int_0^\infty e^{-z} \; dz = 1 \; ,$$

so

$$\nu_{\hat{y}} = \frac{1}{2\pi} \frac{\sigma_{\dot{y}}}{\sigma_y} e^{-\frac{1}{2}(\hat{y}/\sigma_y)^2} = \nu_0 \; e^{-\frac{1}{2}(\hat{y}/\sigma_y)^2}$$

where ν_0 is the zero up-crossing rate (corresponding to $\hat{y} = 0$).

16 Distributions of Gaussean Random Processes

- The process $Y(t)$ is Gaussean, $Y \sim N(0, \sigma_y^2)$
- The envelope of the process $R(t)$ is Rayleigh distributed,

$$f_R(r) = re^{-r^2/2} \quad (r > 0)$$

- The peaks of the process $P(t)$ are exponentially distributed,

$$f_P(p) \approx \frac{\nu_{\hat{y}}}{\nu_0} = e^{-r^2/2} \quad (r > 0)$$

- The distribution of the maximum value of $Y(t)$ within a specified time T is an extreme type I (Gumbel) distribution. Defining $N_{\hat{y}}(T)$ as the number of upcrossings during a time interval T, it is Poisson-distributed with a mean rate $\nu_{\hat{y}}$.

$$\text{Prob}[\max |Y(t)| \le \hat{y}] = \text{Prob}[N_{\hat{y}}(T) = 0] = e^{-\nu_{\hat{y}} T} = \exp[-\nu_0 T \exp[-(1/2)(\hat{y}/\sigma_y)^2]$$

17 First Passage Statistics

To close, we consider a very practical problem [14]. What is the probability that the process $Y(t)$ will not cross a threshold $\hat{y}$ during an interval $0 \le t \le T$? The key result is that this probability is exponentially-distributed,

$$\text{Prob}[Y(t) < \hat{y} \mid 0 \le t \le T] \approx A \exp[-\alpha T]$$

where the coefficient A is the probability that the value at $t = 0$ is less than the threshold,

$$A = \text{Prob}[Y(0) < \hat{y}]$$

For $\hat{y} \gg \sigma_y$, $A \approx 1$ and $\alpha \approx 2\nu_{\hat{y}}$. More accurately, defining the peak response factor $r = \hat{y}/\sigma_y$,

$$A = \text{Prob}[Y(0) < \hat{y}] = 1 - \exp[-r^2/2]$$

and

$$\alpha = 2\frac{\nu_{\hat{y}}}{A}\left(1 - \exp\left[-\sqrt{\pi/2}\ \delta^q\ r\right]\right)$$

where $q \approx 1.2$, and δ is the *bandwidth factor*, which may be computed from the spectral moments of $S_{Y,Y}(f)$, which, in turn, may be computed from the solutions to Liapunov equations.

References

[1] Bendat, J.S. and Piersol, A.G., *Random Data: Analayis and Measurement Procedures*, 4th ed. Wiley 2010.

[2] Childers, D.G., (ed.) *Modern Spectrum Analysis*, IEEE Press, 1978.

[3] Clough, R., and Penzien, J., *Dynamics of Structures*, 2nd ed., CSI Press, 2003. (Ch. 20-21)

[4] Gavin, H.P., Fourier Series, Fourier Transforms, and Periodic Response to Periodic Forcing, CEE 541 course notes, 2018

[5] Gade, Svend, and Herlufsen, Henrik, "Windows to FFT Analysis," *Sound and Vibration* March 1988: 14-22.

[6] Harris, Fredric J., "On the Use of Windows for Harmonic Analysis with the Discrete Fourier Transform," *Proc IEEE* 46(1) (1978) : 51-83.

[7] Lindberg, Craig R., and Park, Jeffrey, "Multiple-taper spectral analysis of terrestrial free oscillations, Part II," *Geophysical Journal of the Royal Astronomical Society,* 91 (1987):795-836.

[8] Lutes, L, and Sarkani, S., *Random Vibrations*, Elsevier 2003.

[9] Park, Jeffrey, Lindberg, Craig R., and Thomson, David J., "Multiple-taper spectral analysis of terrestrial free oscillations, Part I," *Geophysical Journal of the Royal Astronomical Society,* 91 (1987):755-794.

[10] Press, W.H., Flanner, W.H., Teukolsky, S.A., and Vetterling, W.T., *Numerical Recipes in C: The Art of Scientific Computing*, 2nd ed., 1992. (Ch. 13)

[11] Rocklin, G. Thomas , Crowley, John , Vold, Havard , "A comparison of H_1, H_2, and H_v frequency response functions," *Proceedings of the 3rd international Modal Analysis Conference,* Volume 1, Pages 272-278, 1985.

[12] Shinozuka, Masanobu, and Deodatis, George, "Simulation of stochastic processes by spectral representation," *Applied Mechanics Reviews,* 44(4) (1991): 191-204.

[13] Thompson, David J., "Spectrum Estimation and Harmonic Analysis," *Proc. IEEE* 70(9) (1982):1055-1096.

[14] Vanmarcke, Erik, "On the Distribution of the First-Passage Time for Normal Stationary Random Processes," *J. Applied Mechanics*, 42 (1975):215-220.